US Department of the Interior
National Park Service
National Center for
Preservation Technology and Training
Publication No. 1998-1l

Physical and Chemical Processes of Soiling and Washoff at the Cathedral of Learning.

Progress Report for the National Park Service
U.S. Department of the interior
Cooperative Agreement 1443CA001960035
with Carnegie Mellon University

Report Authors

Graduate Students:	Vicken Etycmezian Ross Strader
Faculty:	Cliff Davidson Susan Finger
Undergraduate Students:	Stephannic Behrens Thomas Curry Ivan Locke Preshanth Mekala John Murray Karen Pinkston Warinthorn Songkasiri Jiyoung Lee

Department of Civil and Environmental Engineering
Carnegie Mellon University
Pittsburgh, PA 5213

November 1997

Funding for this report was provided by the National Park Service's National Center for Preservation Technology and Training, Natchitoches, Louisiana. NCPTT promotes and enhances the preservation of prehistoric and historic resources in the United States for present and future generations through the advancement and dissemination of preservation technology and training.

Table of Contents

LIST OF FIGURES

LIST OF TABLES

CHAPTER 1: INTRODUCTION

Sensitive building materials such as calcareous stone are subject to accelerated deterioration by several agents. These may be physical processes such as freeze-thaw cycles, chemical processes such as reaction with sulfur dioxide gas, or biological processes such as attack by microorganisms. We are now beginning to understand some of these processes though our knowledge is very limited.

This project is oriented toward obtaining an improved understanding of pathways for air pollution damage to limestone buildings. In particular, we have been studying some of these pathways at the Cathedral of Learning, a 42-story limestone building on the University of Pittsburgh campus in Pittsburgh, Pennsylvania. Although the focus has been on this building, the larger goal of this project is to extend experimental and modeling results to other historical buildings in need of preservation. Such information can help conservators who are deciding on a best course of action for a deteriorating building. e.g. cleaning, consolidation, or treatment.

Continuing studies within the Cathedral of Learning project can be classified into three Phases. Phase I consists of on-site measurements of atmospheric pollutant concentrations and deposition. In Phase II. a computer program is used to model the airflow around the Cathedral. Model results can be used to study mixing in the vicinity of the Cathedral or as input parameters for later modeling efforts. Finally. Phase III includes development and testing of mathematical models that describe physical events such as surface rain washing and mass transfer of atmospheric pollutants to building surfaces. In addition to the three Phases, several long-term undergraduate projects are in progress. These include developing a computer database for storage of project data, photo-documenting current soiling patterns on the Cathedral. measuring vertical wind speeds near the walls of the Cathedral, and developing devices for measurement of rain flux to the building walls.

This report summarizes the work conducted on the Cathedral of Learning project during the period November 15, 1996 to November 15. 1997. Each of the three Phases described above is represented in the report. Chapter 2 contains experimental procedures and a very brief summary of results for two types of samples that were obtained at the Cathedral Airborne particles collected on polycarbonate filters and particles deposited on vertical surrogate surfaces Chapter 3 discusses modeling of airflow and trajectories of individual raindrops near the Cathedral. In this chapter we first summarize a portion of the relevant literature. Second, we give a preliminary outline of the steps we intend to take for modeling airflow around the Cathedral. Third, we present a simple model

for the trajectory of an individual raindrop in the flow field of a building. A brief summary of the fill report is given in Chapter 4. Finally, Appendix A contains a revised manuscript summarizing results from measurements of vertical gradients of airborne pollutant concentrations and deposition fluxes. This manuscript has appeared in preliminary form in a previous report for this project (Elycmezian et al., 1996). The revised version was submitted for publication to the Journal of the American Institute for Conservation on November 11, 1997.

CHAPTER 2: BACKGROUND AND PROCEDURES FOR SEM ANALYSIS OF PARTICLES AT THE CATHEDRAL OF LEARNING

2.1 INTRODUCTION

Damage to calcareous building stone can occur by gaseous species as well as by particles emitted from anthropogenic activities. Damage by particles can occur through two pathways. First, deposition of particles may cause surface soiling. Second, deposited particles can catalyze chemical reactions of some gaseous species, resulting in accelerated stone deterioration rates. As part of an ongoing investigation of damage and soiling at the Cathedral of Learning, on-site experiments have been conducted with the goal of characterizing both airborne particles and particles that deposit to surrogate vertical surfaces.

Over the course of the 1995-96 fiscal year, experiments were conducted at the Cathedral of Learning during four time periods, fall 1995, and winter, spring, and summer 1996 (Table 2.1). These experiments were intended to elucidate vertical gradients of airborne concentrations of some important pollutants: SO_2 gas. SO_4^{2-} particles, total NO^{3-} (HNO_3 gas and NO^{3-} particles), elemental carbon particles, particle number >0.5 μm and particle number >5μm. Vertical gradients of SO_2 deposition were also investigated with the aid of surrogate surfaces. Details of these experiments were summarized in a manuscript that has been submitted to the Journal of the American Institute for Conservation (JAIC) (Appendix A). During the experiments of the spring and summer of 1996, samples were also collected for particle analysis by scanning electron microscopy (SEM) with energy dispersive spectroscopy (EDS). Two types of samples were collected. First, airborne particles were sampled using a poiycarbonate membrane filter. Second, vertical deposition of airborne particles was sampled by using strips of adhesive carbon tape as surrogate surfaces. These two sample types are different from those summarized in the JAIC manuscript; whereas in the latter case bulk chemical analyses were used to estimate airborne pollutant concentrations and deposition, in the former case large numbers of particles were analyzed individually in order to estimate particle size distributions and particle chemical compositions.

The experimental protocol used for obtaining and analyzing airborne particles and particles deposited to surrogate surfaces is presented below. Some preliminary results are also presented. The analysis of these samples by SEM/EDS is not yet complete; when completed, the results will be summarized in a manuscript for publication. intended to be a companion paper for the manuscript that has already been submitted to JAIC.

2.2 BACKGROUND

Particles in many size ranges and various chemical compositions may be suspended in the atmosphere at any given time. Their presence becomes relevant to building stone deterioration when they deposit on the building walls and alter the appearance or chemical characteristics of the surface. Several authors have reported that soiling of a building surface may be caused by biological growth (e.g. Young, 1996; Freemantle, 1996; and Wilmzig and Bock, 1995) as well as particle deposition. Soiling at the Cathedral of Learning is most likely a result of the latter (see Appendix A). Therefore, the work presented in this chapter pertains only to particles.

The deposition of particles is complicated, in part because many of the relevant processes occur very close to the surface where measurement of parameters may be difficult. Davidson and Wu (1990) give a review of literature pertaining to dry deposition of particles. Seinfeld (1986), Flagan and Seinfeld (1988), and Friedlander (1977) may be consulted for an overview of the physical and chemical characteristics of airborne particles.

Several investigators (Nord et al. 1994; Camuffo et al., 1982; Amoroso and Fassina, 1983; and Sabbioni, 1994) have reported a correlation between soiling of a building wall and the presence of particles on the stone surface. McGee (1997) obtained 38 surface crust samples from the walls of the Cathedral of Learning for analysis by SEM/EDS. Results of her study suggested that high concentrations of atmospheric particles in the surface crust were responsible for the black color on soiled regions of the walls. McGee reported that these particles were spherical and rich in Al, Si, and Fe compounds. The morphology and composition are consistent with fly ash particles.

In addition to soiling the walls of stone buildings, airborne particles may also assist in the formation of gypsum ($CaSO_4$). Soot, transition metal oxide, and fly ash particles have been suspected of catalyzing the oxidation of SO_2 to SO_4^{2-} (Hutchinson et al., 1992). Hutchinson et al (1992) were able to Show that transition metal oxides

do enhance the formation of gypsum in pure $CaCO_3$ samples. However, they report insignificant increases in sulfation rates when samples of limestone were seeded with metal oxide or fly ash particles. On the other hand, Del Monte et al, (1981) noticed that gypsum crystals tended to grow adjacent to carbonaceous particles whereas re precipitated calcite crystals did not exhibit this trait. The findings of these authors were based on SEM/XRD analyses of surface crust samples that were obtained from numerous marble and limestone monuments in Northern Italy**.**

2.3 EXPERIMENTAL

Airborne particles were sampled on the fifth floor, sixteenth floor, and roof of the Cathedral of Learning, while deposition of particles to surrogate surfaces was only measured on the fifth and sixteenth floors. Since the collection of these samples was concurrent with the collection of the samples for bulk chemical analysis that were presented in the JAIC manuscript, many of the handling procedures were also identical. Therefore, we confine the discussion here to elements of the experimental protocol that differ from those already outlined and refer the reader to Appendix A for additional details.

The staged filterpack system used for measuring airborne concentrations of the chemical species (SO_2 gas, SO_4^{2-} particles, total NO_3^-, and elemental carbon particles) was modified to allow for the collection of airborne particles: Quartz fiber filters (Pallflex 2500 QAT-UP) used to sample elemental carbon particles in fall 1995 and winter 1996 were replaced with polycarbonate membrane filters (Costar Nuclepore PC-MB-47mm, 0.4 μm pore size) in spring and summer 1996. The same stainless steel filterpacks (Millipore XX50-047-10, open-faced) that were used with the quartz filters were also used with the polycarbonate filters. In addition to switching filter types, during the summer 1996 sampling period, a metering valve (Hoke 1656 G4YA) was installed inline with the polycarbonate filter to limit the flow to 0.2 liters per minute. The metering valve was installed because samples that were obtained at higher flowrates in the spring were loaded with too many particles for accurate analysis by SEM/EDS.

During the spring and summer 1996 sampling periods, each lasting four weeks, samples of airborne particles were collected on a weekly basis. Two replicate filterpacks contain polycarbonate filters were used on

each floor where airborne particles were sampled. Fitterpacks were installed on air sampling towers at a height of meters Weekly sample changes lasted approximately two hours. On each floor, sample changes were comprised of the following steps:

1. Measuring the flowrates through the two replicate polycarbonate filters that had been collecting particles for the previous week ("exposed" samples)
2. Disconnecting the two "exposed" samples
3. Installing and connecting one field blank
4. Allowing air to flow through the field blank for three minutes in order to account for particles that may have become suspended during sample changes
5. Measuring the flowrate through the field blank
6. Disconnecting the field blank
7. Installing and connecting two filterpacks containing "fresh" polycarbonate filters
8. Measuring the flowrates through the "fresh" polycarbonate filters

When sample changes were complete, "exposed" samples and field blanks were returned to the lab where polycarbonate filters were stored in 47 mm polypropylene petri dishes until the time of analysis.

Flowrates through the polycarbonate filters were set very low (~0.2 liters per minute) during the summer 1996 experiments. Consequently, it was not possible to use a standard dry test meter since time periods required for accurate flowrate measurement were too long. Therefore, volumetric displacement measuring devices were developed. Plastic wrap-coated rubber stoppers were placed on either end of a 2.5 meter-long piece of flexible tubing. This assembly was used to connect the open face of the filterpack to a clear plexiglass pipe, (ID = 4.5 cm). The pipe was partially immersed in a five gallon polycthylene bucket containing deionized (DI) water (Figure 2.1). Plexiglass pipes were marked at two points, with the volume between those points corresponding to 0.2 liters. To measure the flow rate, 1) the filterpack was connected to the plexiglass pipe, 2) a stopwatch was started when the water level in the pipe reached the first marked point and 3) the stopwatch was stopped when the water level reached the second marked point. One volumetric displacement measuring device was constructed for each floor.

Each device was laboratory tested against a dry test meter (Singer DTM- 115). In these laboratory tests, the dry test meter was allowed to operate for long periods of time in order to obtain accurate flow rates. In all cases, discrepancies between flowrates obtained with a volumetric displacement device and the dry test meter never exceeded 2%.

Deposition of particles was sampled using adhesive carbon tape surrogate surfaces (Ladd Research Company) at ten locations on the fifth floor and six locations on the sixteenth floor (Figure 2.2). These surrogate surfaces had dimensions of 4.7 cm by 2.0 cm. With one small piece of duct tape on each end, surrogate surfaces were attached to a PVC backing in the shape of a 90º corner which was, in turn, permanently anchored to the wall of the Cathedral of Learning (Figure 2.3). The backing had two functions: 1) To provide a surface that duct tape can adhere to and 2) to protect the carbon tape from raindrops that would otherwise interfere with deposited particles.

Sample changes of surrogate surfaces occurred weekly during the spring and summer 1996 experiments, On each floor, sample changes were comprised of the following steps:

1. Removing the surrogate surfaces that had been exposed for a week from the PVC backing. The duct tape on the outer edges of each surrogate surface was used to fasten the sample to the bottom of a 125 mm polypropylene petri dish. Petri dishes were sealed with tape and placed in a clean polyethylene bag. Surrogate surfaces remained in petri dishes until the time of analysis.
2. Exposing one field blank for three minutes
3. Removing the field blank and placing it in a petri dish
4. Attaching fresh strips of carbon tape to the PVC backing using small pieces of duct tape.

2.3.1 SEM/EDS ANALYSIS

Sample analyses by SEM/EDS have been in progress since the samples were collected in spring and summer 1996. To date, 94 of the 108 samples (36 airborne particle and 72 adhesive carbon tape) have been analyzed once. We intend to perform replicate SEM/EDS analyses for 24 of the 72 adhesive carbon tape samples.

Since two replicate airborne particle samplers were used on each floor, replicate SEM/EDS analyses for these samples was deemed unnecessary.

Sample analysis is performed using a Personal Scanning Electron Microscope (PSEM), developed by the R.J. Lee Group, Export, PA (Schwoeble et al., 1990). Figure 2.4 shows the basic operational principle of an SEM. In short, a scanning electron microscope focuses a beam of electrons on an object and analyzes the signals produced by the interaction between the electron beam and the object. Three types of signals are produced by the interaction: secondary electron (SE), back-scattered electron (BSE), and x-ray. To determine the composition of the object, an energy dispersive spectrometer (EDS) is used to analyze the x-ray signal. Figure 2.5 is an example of the spectrum of a predominantly aluminum silicate particle. The amplitudes of the various peaks, are indicative of the elemental composition.

The PSEM belongs to a class of instruments known as CCSEMs (computer controlled SEMs). The advent of CCSEM has made it possible to use the SEM/EDS technique to analyze large numbers of particles collected on a surface such as a filter or a surrogate deposition surface. Once the PSEM has been set up correctly, it is able to scan the sample for particles and perform analysis on those particles with little operator intervention. Whereas manually analyzing 500 particles per sample would be time-consuming. CCSEMs can complete the task in less than an hour.

In preparation for analysis, samples must undergo two procedures. First, they must be mounted onto small stubs that can be loaded onto the sample stage of the PSEM. Stubs consist of thin carbon disks (diameter = 2 cm) attached to small round metal platforms. Petri dishes containing airborne particle samples (polycarbonate filters) are opened and a small portion of the filter (~1 cm^2) are affixed to a stub using colloidal graphite suspension. Filters are cut with scalpels and handled with clean tweezers. For adhesive carbon tape samples, petri dishes are opened and a small portion of the sample (~1 5 cm^2) is removed, again using scalpel and tweezers. Each sample is then affixed to a stub using double-sided carbon tape.

Second, both airborne particle and adhesive tape samples must be carbon-coated to prevent buildup of charge that would result in degradation of image resolution. The fine carbon coating over the sample acts as a shunt that disperses the negative charge created by the electron beam. Carbon coating involves placing the sample

in a vacuum chamber and vaporizing a short length of carbon rod (1 cm) over the sample. This covers the entire sample with a uniform layer of carbon.

Once a sample is carbon coated, it is ready to be placed in the PSEM. Typically a batch of four samples is loaded onto the stage for analysis. The sample chamber is then brought to a vacuum and the electron beam is turned on. Several parameters are set before the PSEM can start automated analysis. The stage is moved manually and for each sample, four boundary points are entered into the PSEM. The appropriate focus setting is specified at each point. These boundary points comprise the vertices of the quadrilateral enclosing the target area for analysis. Brightness and contrast levels are set to differentiate particles from the background. Finally, the threshold for detection must be specified so that the PSEM only analyzes particles with emissions higher than a Set criterion. Threshold levels consist of a “detect” setting as well as a “measure” setting. “Measure” allows the user to set the base level from which the PSEM will calculate the amplitude of the peaks. In effect, this is equivalent to subtracting background noise from the sample signal. The “detect” levels are set higher than “measure” levels. The PSEM analyzes a particle only if emissions from that particle are higher than the “detect” level. After all parameters have been specified, automated analysis may be started. All particles with average diameters between 0.2 μm and 100 μm emitting ,x-rays higher than the “detect” level are analyzed for chemical composition. Analysis results for each particle, including size and emission spectra are stored by the PSEM for later data analysis.

2.4 BRIEF SUMMARY OF OBSERVED PARTICLE COMPOSITION CATEGORIES AND AVERAGE SIZE

Analysis of samples by SEM/EDS is still underway. Upon completion of analysis. data sets including airborne and deposition particle size distributions will be compiled and discussed more rigorously in a future report.

The software for the PSEM allows for particles to be classified into different categories based on the chemistry of the particle. These categories are specified for the PSEM by a set of rules which are applied to the emission spectra of a particle. Emissions of x-rays by an element constitute a certain percent of emissions by all elements that are found in the particle. Thus, logical operators may be used in conjunction with percent emission

values to cluster a set of particles with similar composition into one category. At least three different categories of particles have been identified for both airborne and deposition samples. They are: 1) calcium, sulfur and silicon rich (Ca-S-Si), 2) aluminum, silicon, and iron rich (Al-Si-Fe), and 3) calcium and magnesium rich (Ca-Mg). The majority of particles (~75%) can be classified into one of these categories. Since samples are carbon coated before analysis by SEM/EDS, chemical compositions of elemental and organic carbon particles cannot be obtained. Thus, those particles are not considered in this study.

In addition to chemical composition, particles may also be classified by size ranges. The size of a particle is often closely linked with its origin (source) as well as chemical composition. In general particles found on airborne filters are smaller than those found on surrogate deposition surfaces. Whereas in the former case average particle size (diameter) based on number concentrations is between 1 and 2 μm, in the latter case average sizes are between 3 and 6 μm. This discrepancy may be due to some particle sizes depositing onto the vertical surfaces more readily than others. Such a phenomenon is well-documented for deposition to horizontal surfaces (e.g. Friedlander, 1977; Flagan and Seinfeld, 1988). Completion of sample analyses and scrutiny of the data may lead to a similar conclusion for vertical surfaces.

Table 2.1

Sampling Schedule at the Cathedral of Learning[a].

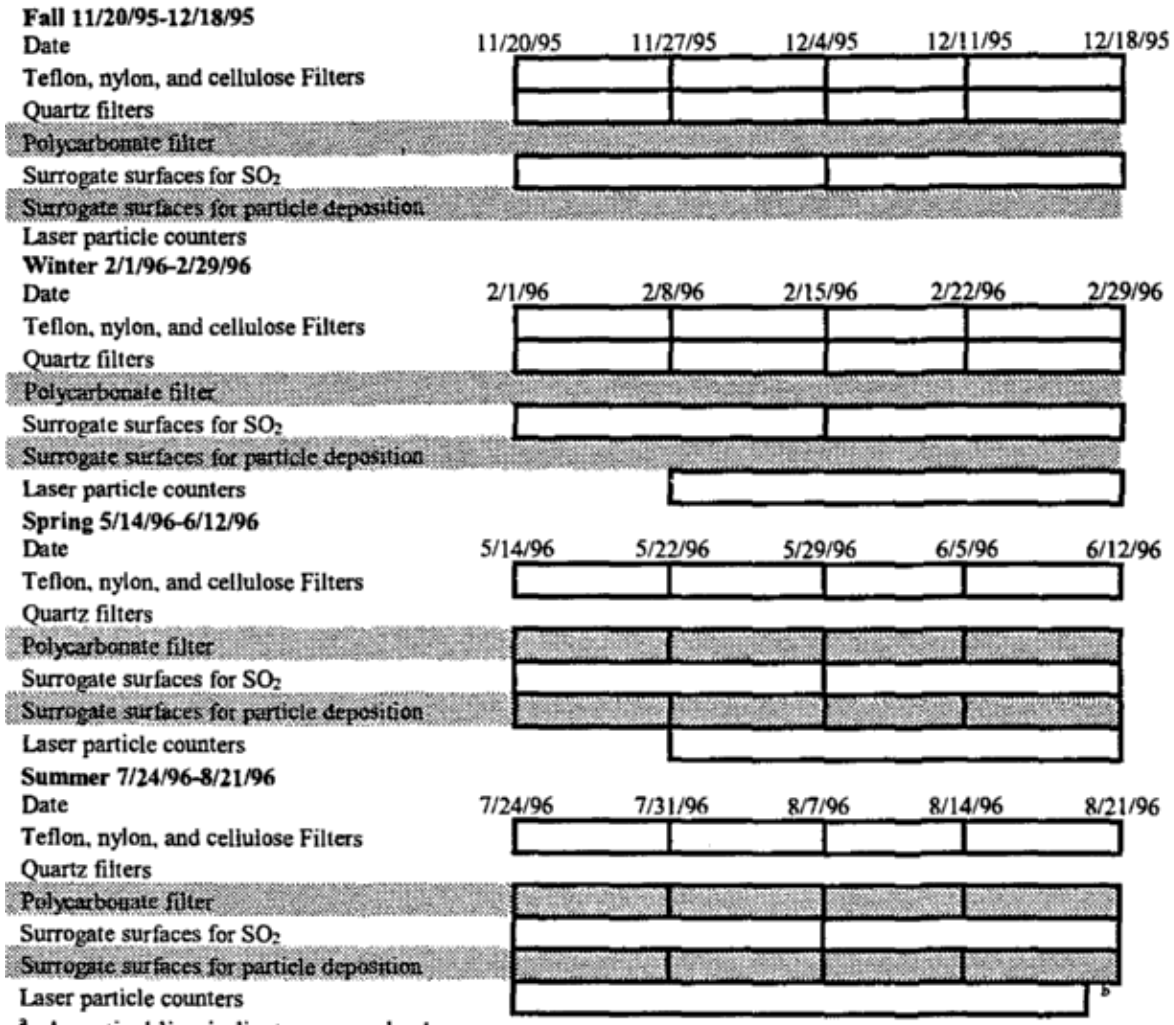

[a] A vertical line indicates a sample change.

[b] No data past 8/16/96

Figure 2.1. Volumetric Displacement Device.

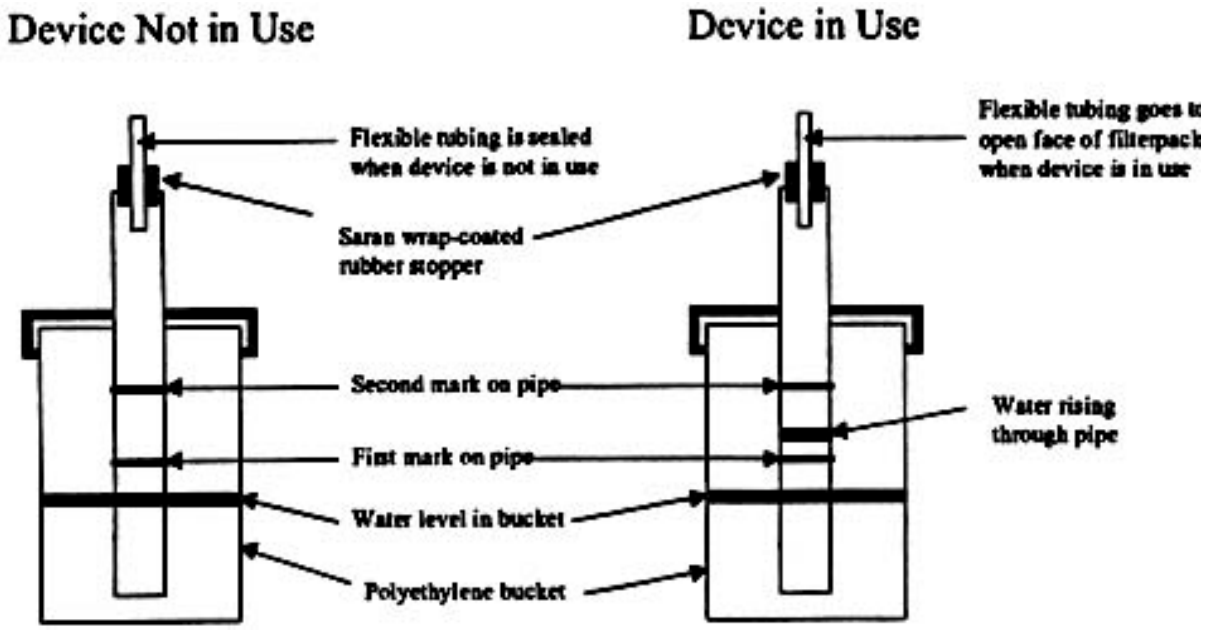

Figure 2.2. Sampling Locations at the Cathedral of Learning.
Locations 5-7 and 5-10 were not used

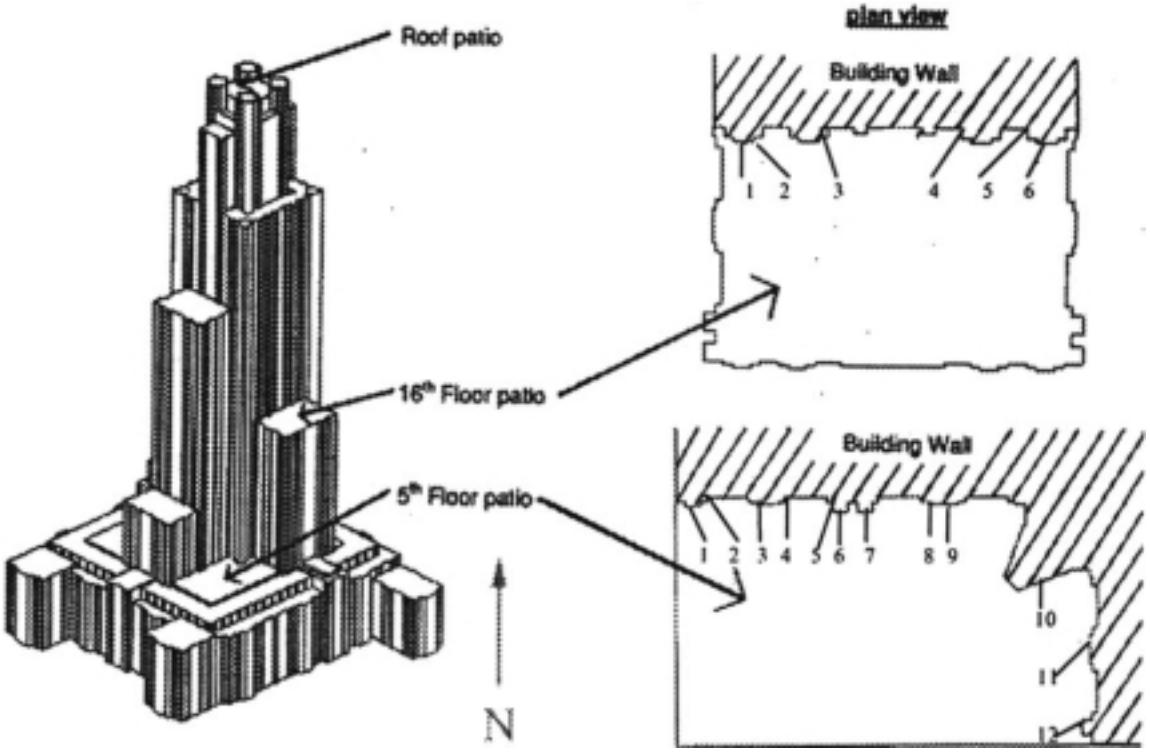

Figure 2.3. Surrogate Vertical Surfaces for Particle Deposition.

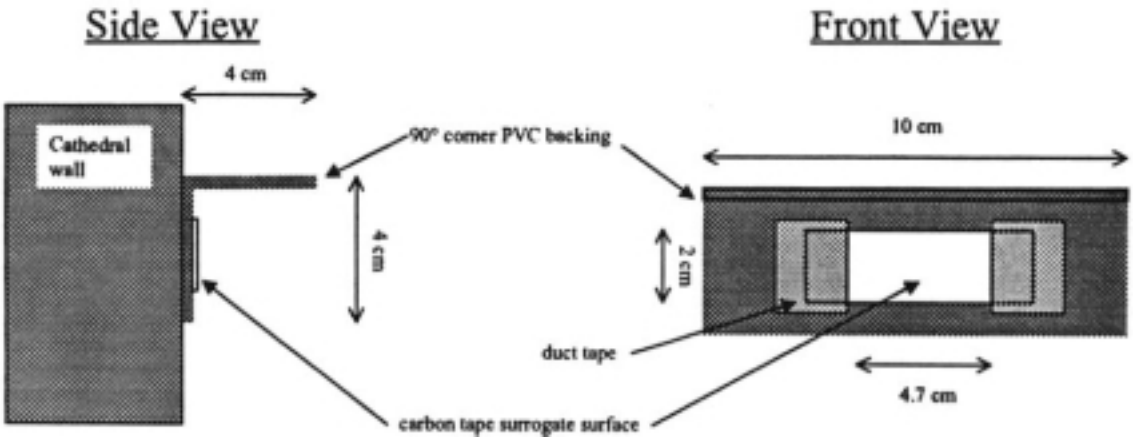

Figure 2.4. Schematic of Scanning Electron Microscope.

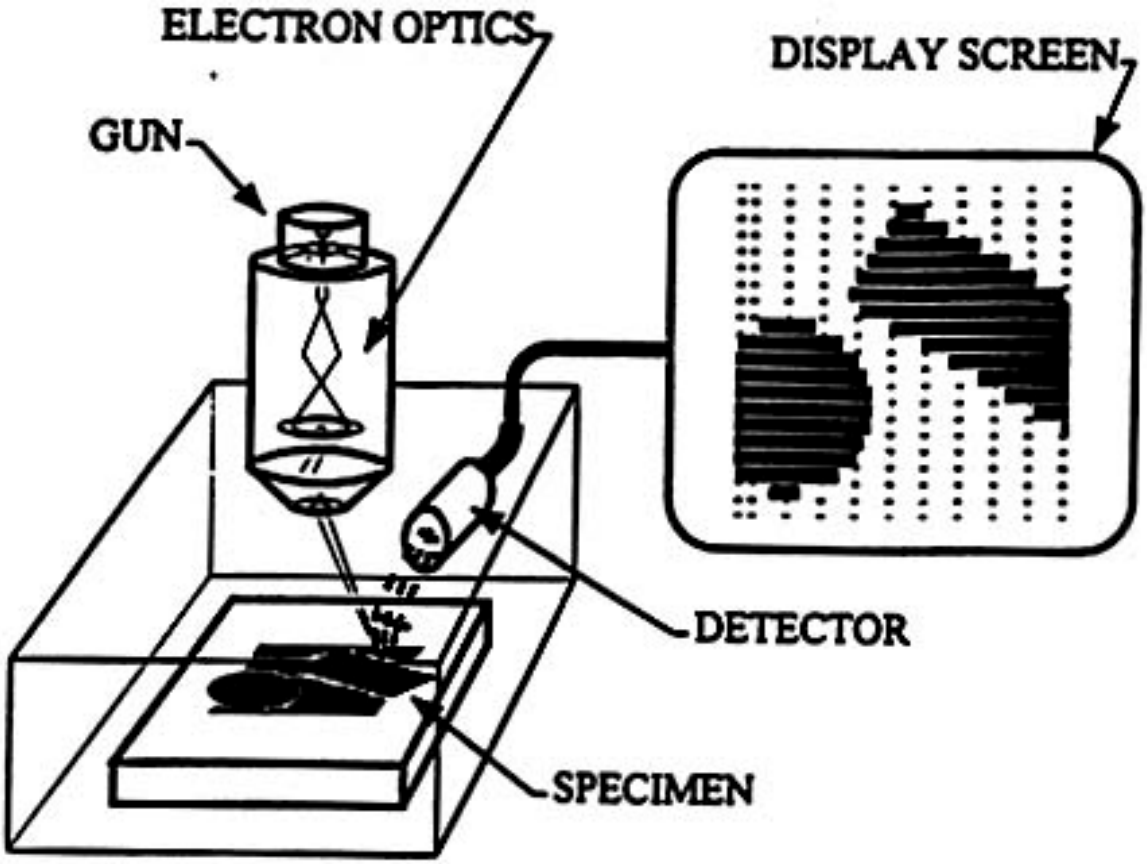

Figure 2.5. Scanning Electron Micrograph and Emission Spectrum for a Predominantly Aluminum Silicate Particle.

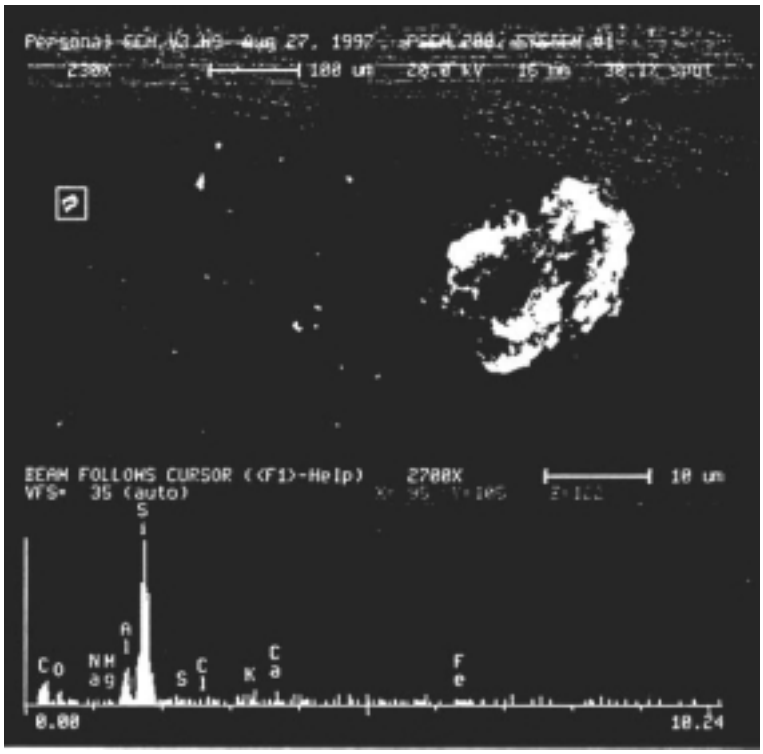

CHAPTER 3: AIRFLOW AND DELIVERY OF RAIN TO THE CATHEDRAL OF LEARNING

3.1 INTRODUCTION

Estimating the extent to which surfaces, such as walls of *a* building, are exposed to rain is essential for understanding the deterioration mechanisms for those surfaces. This is especiafly true for historic calcareous stone structures since delivery of rain may have implications for the rate of dissolution of calcite and gypsum (Mossotti and Eldeeb, 1994), productivity of harmful microorganisms (Bock and Sand, 1993), and appearance of soiling patterns (Hamilton and Mansfield, 1993). Experiments conducted at the Cathedral of Learning in 1995-1996 underscore the importance of exposure of a limestone building to rain (Etyemezian et al., 1997, included in Appendix A).

In general, the airflow near a solid obstacle such as a building has a profound impact on the trajectory of an individual rain drop Wind approaching an obstacle such as a building must be diverted, and this results in a change in the local wind velocities and causes a difference between the velocity of a falling rain drop and the localized wind patterns. Because of friction and aerodynamic pressure, the rain drop experiences a drag force. Qualitatively, the drag force retards the motion of the drop towards the building Since most rain drops have diameters greater than ~0.2 mm (Seinfeld, 1986), and therefore also have considerable inertia, the drag force may not be sufficient to redirect the rain drop around the building. Consequently, some drops may impinge on vertical surfaces such as walls.

This chapter is divided into three sections. First, we discuss the characteristics of airflow around buildings in Section 3.2, with special focus on the distinctive features of the flow field Wind tunnel studies have been a major source of information on this topic. Therefore, a brief discussion on scaling parameters in wind tunnel experiments is also included. Second, we give an outline of a computer model for rain delivery to a building (Section 3.3). The model is divided into two parts, airflow simulation and rain drop trajectory calculation. Although this model is intended for use at the Cathedral, the formulation

is not specific to any particular building Third, the contents of the chapter are summarized in Section 3.4.

3.2 AIRFLOW AROUND A BUILDING

Airflow around buildings has received considerable attention in recent decades because of the implications for the dispersion of pollutants emitted from nearby sources (e.g. Robins and Castro, 1977a; Ogawa and Oikawa, 1983a; Snyder and Lawson, 1976). One of the primary concerns is the entrainment of pollutants in the building wake cavity and the downwash of an elevated plume as a result of the cavity. Consequently, much of the research has been geared toward a better understanding of the flow separation that occurs at the leading edge as well as an estimation of the size of the building wake cavity. Hosker (1984) has provided a comprehensive review of studies conducted in this area of research through 1981.

The airflow over a bluff body, such as a building, is very complex. As a result, most studies on such airflows have employed wind tunnel studies rather than field measurements. Figure 3.1 illustrates some of the main features of the flow field. Typically, the flow of a fluid over a bluff body at high Reynolds numbers can be divided into four regions: the windward faces, roof, near wake, and far wake. The windward faces are expected to receive the most rain. Therefore, flow patterns in this region are very important. Although we are not directly concerned with airflow on the roof, the cavity formed in this area is closely linked with the flow over the windward face. Likewise, flow patterns in the near wake of buildings are not directly pertinent to the impingement of rain drops on windward faces. However, the cavity of the near wake is a major feature of flow in the building envelope and therefore requires some attention. Characteristics of the far wake are not discussed here. The discussion here focuses on incident flow normal to one side of the building, although we briefly discuss the effect of incidence angle at the end of the section.

3.2.1 WIND TUNNEL MODELING

In order for wind tunnel data to be relevant to field conditions, certain characteristics of the boundary layers in the atmosphere and the wind tunnel should be similar For example, we can assume that the velocity profile in the region of the boundary layer to be modeled can be expressed as:

$$U / U_r = \left(\frac{z}{z_r}\right)^n \tag{3.1}$$

where U is the velocity at height z, and U_r and Z_r are the reference velocity and reference height, respectively. The boundary layers in the atmosphere and wind tunnel are considered similar if the exponent n in Equation 3.1 is nearly the same for both situations *(*Plate*,* 1982). If the building height h is larger than the atmospheric boundary layer height δ or if the influence of the airflow around the building is not contained within the boundary layer, then there is an additional criterion that h/δ for the building and for the model of the building in the wind tunnel should be similar. Boundary layer similarity is usually achieved in the wind tunnel by placing appropriate roughness elements upstream of the model building.

Exact dynamic similarity can only be realized when the relevant dimensionless groups are matched identically in the atmospheric and simulated flow. Some of these groups include the Rossby number, Reynolds number, Richardson number, Prandtl number, and Eckert number. Of all these parameters, only the Reynolds number Re has a significant effect in neutrally stratified boundary layer flow. Here $Re= U_r \bullet L_r / \nu$, where U_r and L_r are respectively, the reference velocity and length scale, usually taken as the building height, and ν is the kinematic viscosity of air. Building models used in wind tunnels are often at a scale of 1:1000. If exact Reynolds number similitude is to be achieved, freestream velocities in wind tunnels would have to be about 1000 times the freestream velocities in the atmosphere. Fortunately, for a boundary layer flow, the flow field becomes independent of Reynolds number (Re) above a critical value and the major features of the flow can be captured in a wind tunnel. The critical value needed to achieve Reynolds number independence ~10,000. Several authors discuss dynamic similarity considerations for wind tunnel-simulated flow around buildings (Neff and Meroney 1996; Plate 1982; Snyder and Lawson 1976; Cermak 1976; Castro and Robins 1977; Saathoff et al (1995).

3.2.2 FLOW AND SEPARATION AT TIIE WINDWARD FACE

When a building is immersed in a shear flow, e g. an atmospheric boundary layer, a negative pressure gradient is formed below the front stagnation point. Note that Figure 3.2 shows a small trough in the surface pressure coefficient for the front face of a cube in shear flow (Case B). The flow below this point is directed downwards along the windward wall. The adverse pressure gradient near the ground causes the boundary layer upwind of the building to separate some distance upstream. As a result, a horizontally-oriented standing vortex is formed near the lower half of the windward wall. This phenomenon has been studied and characterized in two-dimensional flows (e.g. Good and Joubert, 1968). In three dimensional flows, the standing vortex is often likened to a horseshoe because of the characteristic shape of the portion that trails off to the sides of the building. The dependence of the size of the standing vortex on parameters such as building geometry and upstream flow conditions has not been well characterized for the three dimensional case. In a wind tunnel study using a power law incident flow (Equation 3 1), Corke and Nagib (1976) were able to show that the height of the boundary between upward and downward directed flows along the windward face increases with n. This suggests that the size of the standing vortex increases with shear in the incident flow.

Another feature of the airflow is the separation that occurs at the top and sides of the windward face. Unlike in the case of rounded objects, boundary layer separation on buildings occurs at sharp edges and is not dictated by an aerodynamic force balance (e.g. Schlicting, 1960). The recirculation zone above the building is often called the roof cavity or roof bubble. Boundary layers separated at the leading edge (edge of roof and windward face) may or may not reattach to the roof depending on the incident flow and the building geometry. Castro and Robins (1977) and Robins and Castro (1977b) report that boundary layers that separate at the windward edges do not reattach to the surface of a cube in uniform flow at zero incidence angle. However, when the incident flow is sheared, i.e. exhibits a velocity gradient in the vertical direction, reattachment is observed for boundary layers separated from the sides of the cube as well as from the leading edge. Based on a review of the literature, Hosker (1979) suggests that in atmospheric flows, i.e. sheared flows, reattachment to the roof will occur if the building length to height L/H ratio is greater than or equal to unity and the building width to height ratio W/H is not much greater than unity.

3.2.3 THE NEAR WAKE REGION

After the flow separates from the windward edges of the building, it may either reattach to the roof or sides, or to the ground at some distance downstream of the building. Reattachment on the roof results in separation from the trailing edge on the leeward side of the building. Consequently, the flow along the leeward face is directed upwards. Near the leeward face, the flow along the ground is directed toward the building. If the boundary layer does reattach to the sides of the building, two vertically oriented counter-rotating vortices are formed at the trailing edges where the flow separates from the sides of the building once again (e.g. Ogawa et al., 1983b). This phenomenon can be seen schematically in Figure 3. 1.

3.2.4 EFFECT OF WIND INCIDENCE ANGLE

Up to this point, the discussion has focused on incident wind normal to a side of the building. Changing the incident wind angle has several repercussions. The majority of information available is for incidence angles of 0° and 45°. It is instructive to highlight some of the major differences in flow patterns between these two cases. Because of the wedge profile of the building in the 45° case, a smaller fraction of the incident flow is diverted over the top of the building as compared with the 0° case. Nevertheless, boundary layer separation does occur at the roof leading edges (Castro and Robins, 1977). Unlike the case of 0° incidence, a separation bubble does not appear on the roof Instead, a pair of counter-rotating vortices are created at the point where the two leading edges meet In this geometry, the separated boundary layer does not reattach to the roof (Hosker, 1984). Reattachment of the boundary layers separated from the roof and side edges does occur on the ground further downstream of the building. However, the pattern of reattachment is quite complex and heavily dependent on the incident wind profile (Ogawa et al, 1983b).

Similar to the case of 0° incidence, 45° incidence results in a pair of vertically oriented counter-rotating vortices at the trailing edges. However, these vortices are much more pronounced in the 45°

case (Ogawa et al., 1983b; Ogawa and Oikawa, 1982). In addition, the vortices, and indeed the entire flow field, are more intermittent, even in the steady flow of a wind tunnel. This intermittence is due to the fact that at 45° incidence, the stagnation point on the windward side is inherently unstable (Castro and Robins, 1977) and has a tendency to fluctuate across the plane of symmetry.

3.3 MODELING APPROACH

The calculation of rain drop trajectories around a building is a two-part process. First, the airflow around the building must be determined. Second, the trajectory of rain subjected to the airflow must be calculated. Other authors have investigated this two part process for various applications. Twohy and Rogers (1993) calculate the delivery of rain drops to sampling instruments on aircraft In a similar study, King and Dujmovic (1987) evaluate the impingement of snow on automobile windshields. However, in both of these studies, the authors use potential flow theory to calculate the flow field, an approach that is not applicable to inherently sheared flows such as in a boundary layer. Lakehal et al (1995) use the k-ε model of turbulence to calculate the mean flow in a two dimensional street canyon and a Lagrangian model to simulate rain drop trajectories. They also incorporate the effect of turbulence using a stochastic method Finally, Choi (1993) uses a similar approach to simulate the trajectories of rain drops around a building. However, he only considers normally incident flow using a generic shape for a building model.

3.3.1 AIRFLOW MODELING

Computational Fluid Dynamics (CFD) has become an increasingly popular method of studying airfiows around and inside building environments (Scholes and Johnson, 1995). Advancements in computing and in numerical techniques have rendered CFD a viable alternative to time-consuming wind tunnel experiments and virtually unaffordable field experiments. In this project, the modeling of airflow around the Cathedral of Learning will be accomplished numerically using the k- ε turbulence model. Initially, the computer model will be run with a basic building shape such as a cube or rectangle. Results from these model runs will be compared with field and wind tunnel data from the literature. Next, the

geometry of the building to be modeled wilt be altered to approach the geometry of the Cathedral of Learning by the addition of smaller cubes and rectangles to the basic building shape.

There are several methods available for modeling turbulent flows numerically. They include direct numerical simulation, one and two equation models of turbulence (Launder and Spalding, 1972), and large eddy simulation (Deardorff, 1970), a combination of the former two In recent decades, a two equation model, k-ε, has emerged as a popular technique for flow simulation. In this model, transport equations for the turbulent kinetic energy (k) and the rate of energy dissipation (ε) are solved in conjunction with the continuity and the Reynolds-averaged steady Navier-Stokes equations. The formulation given by Launder and Spalding (1974) as it appears in Zhou and Stathopoulos (1996) is given below:

$$\frac{\partial U_j}{\partial x_j} = 0 \qquad \text{(3.2)(continuity eqn).}$$

$$U_j \frac{\partial U_i}{\partial x_j} = -\frac{\partial P}{\partial x_i} + \frac{\partial}{\partial x_j}\left[(\upsilon + \upsilon_t)\frac{\partial U_i}{\partial x_j}\right] + \frac{\partial \upsilon_t}{\partial x_j}\frac{\partial U_j}{\partial x_i} \qquad \text{(3.3)(momentum eqn).}$$

$$U_j \frac{\partial k}{\partial x_j} = \frac{\partial}{\partial x_j}\left[\left(\upsilon + \frac{\upsilon_t}{\sigma_1}\right)\frac{\partial k}{\partial x_j}\right] + \upsilon_t \frac{\partial U_i}{\partial x_j}\left(\frac{\partial U_i}{\partial x_j} + \frac{\partial U_j}{\partial x_i}\right) - \varepsilon \qquad \text{(3.4)(k transport eqn).}$$

$$U_j \frac{\partial \varepsilon}{\partial x_j} = \frac{\partial}{\partial x_j}\left[\left(\upsilon + \frac{\upsilon_t}{\sigma_2}\right)\frac{\partial \varepsilon}{\partial x_j}\right] + C_1 \upsilon_t \frac{\varepsilon}{k}\frac{\partial U_i}{\partial x_j}\left(\frac{\partial U_i}{\partial x_j} + \frac{\partial U_j}{\partial x_i}\right) - C_2 \frac{\varepsilon^2}{k} \qquad \text{(3.5)(}\varepsilon\text{ transport eqn).}$$

$$\upsilon_t = C_\mu \frac{k^2}{\varepsilon} \qquad \text{(3.6)}$$

$$P = \frac{\overline{p}}{\rho} + \frac{2}{3}k \qquad \text{(3.7)}$$

$$k = \frac{1}{2}\overline{u_j u_j} \qquad \text{(3.8)}$$

$$\varepsilon = \upsilon \overline{\frac{\partial u_i}{\partial x_j}\frac{\partial u_i}{\partial x_k}} \qquad \text{(3.9)}$$

$U_i \equiv$ mean velocity in x, direction
$u_i \equiv$ fluctuating velocity in x, direction
$P \equiv$ augmented pressure
Þ $\equiv$ mean pressure
$\rho \equiv$ density of air
$k \equiv$ turbulent kinetic energy
$\in \equiv$ rate of energy dissipation
$\nu_t \equiv$ eddy viscosity
$\nu \equiv$ viscosity of air
σ = l.0, σ_2 =1.3,C_μ =0.09,C_1 = 1.44, and C_2 =1.92.

Equations 3 2-5 comprise a system of six equations and six unknowns (Equation 3.3 is actually three equations, one for each of the Cartesian directions). They are solved numerically with the aid of a finite element grid system and a set of boundary conditions. For this project, these equations will be solved with the aid of commercially available software. Two software packages will be evaluated for robustness, ease of use, and post-processing capabilities. These are ANSYS and FLUENT. The better package, overall, will be used.

The computational domain for the flow around buildings (Figure 3 3) requires several different types of boundary conditions. There are those at the inflow, the upper and side boundaries, and the solid boundaries. There is some flexibility in choosing boundary conditions depending on the size of the domain and the characteristics of the flow. At the inflow and upstream boundaries, the conditions for the velocity components, k, and ε (Figure 3.4) are given by an assumed boundary layer profile (Zhou and Stathopoulos, 1996). At the upper and side boundaries, tangential components of velocity, k, and ε are Set to zero (Murakami and Mochida, 1989). On solid boundaries a form of the law of the wall is used (Launder and Spalding, 1974; Patterson and Appelt, 1989; Murakami et al., 1996; Selvam, 1996; Mikkelsen and Livesy, 1995). This boundary condition is based on the assumption that the velocity in the boundary layer formed on a solid wall follows a logarithmic profile. Other researchers (e.g. Lam and Bremhorst, 1979) have attempted to modify equations 3.2, 3.3, and 3.5 so that they apply from the fully turbulent core through the viscous sublayer, thereby eliminating the need to assume a logarithmic profile near the wall.

In its most simplified form, the Cathedral of Learning is a single rectangular structure. Detail can be added to this basic form by appending additional cubic and rectangular pieces. Therefore, the first step is to implement the k-ε airflow model for two basic building shapes, a rectangle and a cube. Mode results for these shapes can then be compared with field and wind tunnel data from the literature. Minson et al, (1995) have provided tabulated velocity information for a cube in a well characterized wind tunnel low. These data are expressly intended for model testing by researchers in computational fluid mechanics. However, airflow modeling results may also be compared with measurements by some of the authors cited above (e.g. Castro and Robins, 1977, Ogawa et al., 1983b; Ogawa and Oikawa, 1982). Once the agreement between the computational model and literature data- for both 0° and 45° incident flows- is acceptable, the geometry of the basic building model can be altered by the gradual addition of detail. At some point, further detail ceases to improve the quality of the results and requires higher computational effort. Thus, the degree of complexity of the model building is not without bounds.

3.3.2 RAIN DROP SIZE DISTRIBUTIONS AND TRAJECTORIES

The equations of motion for a single rain drop can be written as:

$$M\frac{dU_i^p}{dt} = -F_{Di} - M\delta_{ij}g \qquad (3.10)$$

$M \equiv$ particle mass

$U^p_i \equiv$ if particle velocity in x_i direction

$F_{Di} \equiv$ drag force in x_i direction

G ≡ gravitaional constant

$\delta_{if} \equiv$ delta function; δ_{if} , =1 if $I = j$, $\delta_{if} = 0$ if $i \neq$ j.

The form of F_D depends on the relative velocity of the drop in the flow field and the drag coefficient, which is based on the assumed shape of the drop. Note that a rain drop moving through the air experiences aerodynamic pressure forces that can alter its shape. Qualitatively, drops with diameter greater than -200 μm are too large to retain a spherical shape at their terminal velocities. At these large sizes, drops form, on average, a spherical obloid shape as shown in Figure 3.5 (Beard and Chuang,

1987; Ramaswamy, 1979; Reizebos and Epema, 1985). Furthermore, because of perturbations in the airflow at the drop surface, the instantaneous shape may be quite variable (Beard and Chuang, 1987). These complexities coupled with an absence of data on drop shapes at relative velocities different from the terminal velocity require that a simplifying assumption be made. Other investigators have assumed that the drag coefficient for a rain drop is identical to that of a sphere (Lakehal et al., 1995; Twohy and Rogers, 1992) and this assumption Will be adopted for the present model. The resulting equation for F_D becomes:

$$F_{Di} = C_D \pi r^2 \rho \left(U_i - U_i^p\right) \left|U_i - U_i^p\right| \tag{3.11}$$

$C_D \equiv$ coefficient of drag f(Re)

Re sphere Reynolds number = $2r\sqrt{\sum_1^3 \left(U_i - U_i^p\right)^2} \Big/ \upsilon$

$r \equiv$ raindrop diameter

$\rho \equiv$ density of air

$\upsilon \equiv$ kinematic viscosity of air.

The size distribution of rain drops in free fall is determined by the competing processes of drop breakup and coalescence (Brown and Whittlesey, 1992). Larger rain drops have higher terminal velocities than smaller ones. Consequently, collisions between rain drops occur somewhat frequently. On the other hand, large drops are unstable and tend to break up into smaller drops (Alusa, 1975). The result is an equilibrium size distribution similar to the one shown in Figure 3.6. The theoretical model for this size distribution has the attractive property that its shape does not vary with rainfall intensity (Gillespie and List, 1978/1979). However, caution must be exercised before this model is used and a comparison with measured field data is necessary. These data may be obtained either from the literature or from measurements at the Cathedral of Learning.

The possibility of using a disdrometer to sample rain drop sizes is being investigated. A disdrometer is a simple instrument fashioned after a sensitive scale (Loffler-Mang et al., 1996). Individual rain drops impinging on a horizontal plate cause the plate to move slightly (Figure 3.7). A series of springs and inductor coils generate an electrical signal each time the horizontal plate is moved.

The sizes of the impinging rain drops are then deduced based on this signal. At this time, it is unclear if the use of a disdrometer at the Cathedral of Learning is feasible.

3.3.3 RAIN IMPINGEMENT: FIELD DATA

The rain trajectory model is expected to generate three output parameters: the flux of rain to the building surface (measured in units of mass per unit time per unit building surface area) and the normal and tangential impingement velocities for rain drops of different sizes. Development of a device to measure rain flux to the walls of the Cathedral of Learning is currently underway. Sheets of thin PVC at being used as vertical rain collection surfaces on the roof of Porter Hall on the Carnegie Mellon University campus. If these preliminary experiments are successful, then similar devices can be used a surrogate surfaces for incident rain collection at the Cathedral of Learning. Data gathered from these devices can be compared with model predictions.

Rain impingement modeling results can also be compared with soiling patterns directly. For example, the spatial distributions of impingement velocities for individual rain drops can be transformed into distributions of momentum flux to the walls. These can then be compared with observed soiling patterns at the Cathedral of Learning, assuming that regions of high impingement velocities will have greater erosion of surface material and therefore less visible blackness.

3.4 SUMMARY

Results from experiments conducted in 1995-1996 (Appendix A) suggested that the delivery of rain to the Cathedral walls is an important process. Based on these findings, a modeling effort geared toward a better understanding of rain trajectories around buildings, and the Cathedral in particular, has been proposed. The simulation of airflow around a building will be accomplished numerically with the k-ε model for turbulence Initial results, based on simple building geometries, will bi compared with data available from the literature. Degrees of complexity will be added to the geometry subsequently until an optimum level of detail is achieved. Rain trajectories near and around the building model will be calculated based on simple equations of motion and the assumption that drag coefficients

for rain drops are similar to those for a sphere. Rain drop size distributions will be obtained from the literature and, if possible, measured at a location near the Cathedral of Learning. It initial tests are successful, rain fluxes to the Cathedral walls will be measured with PVC surrogate surfaces for rain collection and compared to those from modeling results. Finally, soiling patterns at the Cathedral will be compared with output parameters from the rain trajectory model.

Figure 3.1. Model of Flow Near a Sharp-Edged Three-Dimensional Building in a Deep Boundary Layer. ***Hosker (1984).***

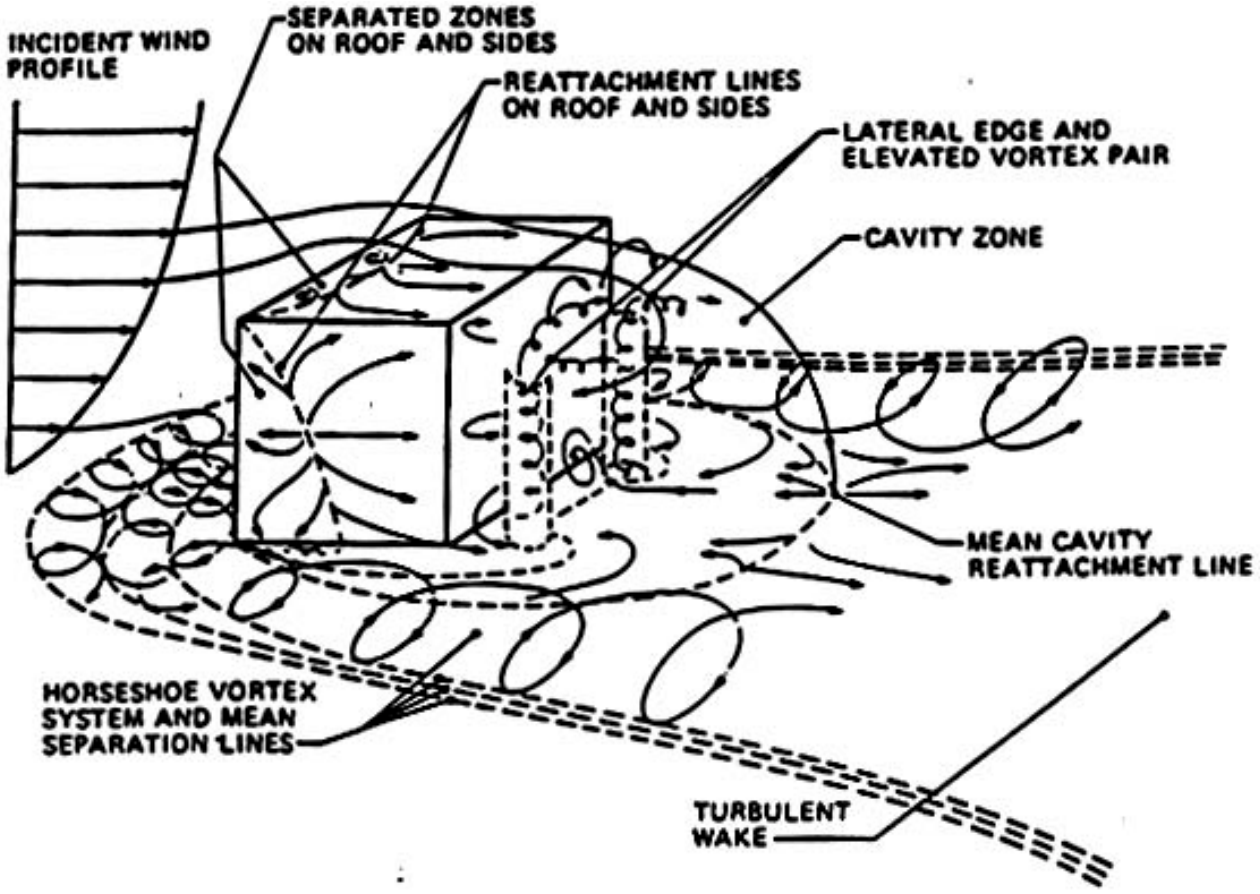

Figure 3.2. Surface Pressure Coefficient on a Cube in a Wind Tunnel. ***Castro and Robins (1977).***

The incident *flow is* uniform in case A and in case B the boundary layer depth is 10 times the cube height.
$c_{pm}(p_s - p_r)/1/2\rho U^2_r$ where p_s , p_r , and U_r are the static surface pressure and the reference pressure and velocity, taken at the wind tunnel exit.

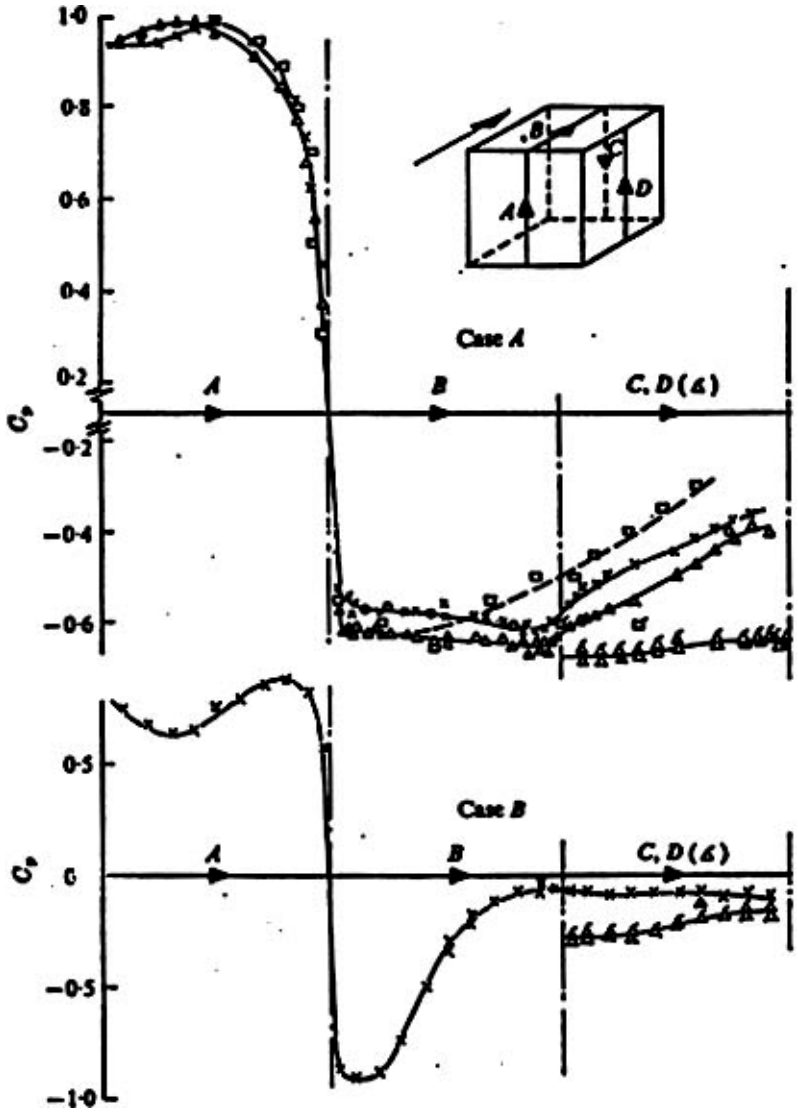

Figure 3.3. Example of Computational Grid System for a Cube in a Boundary Layer. *Zhou and Stathopoulos (1996).*

x, y, and z are the streamwise, transverse, and vertical directions

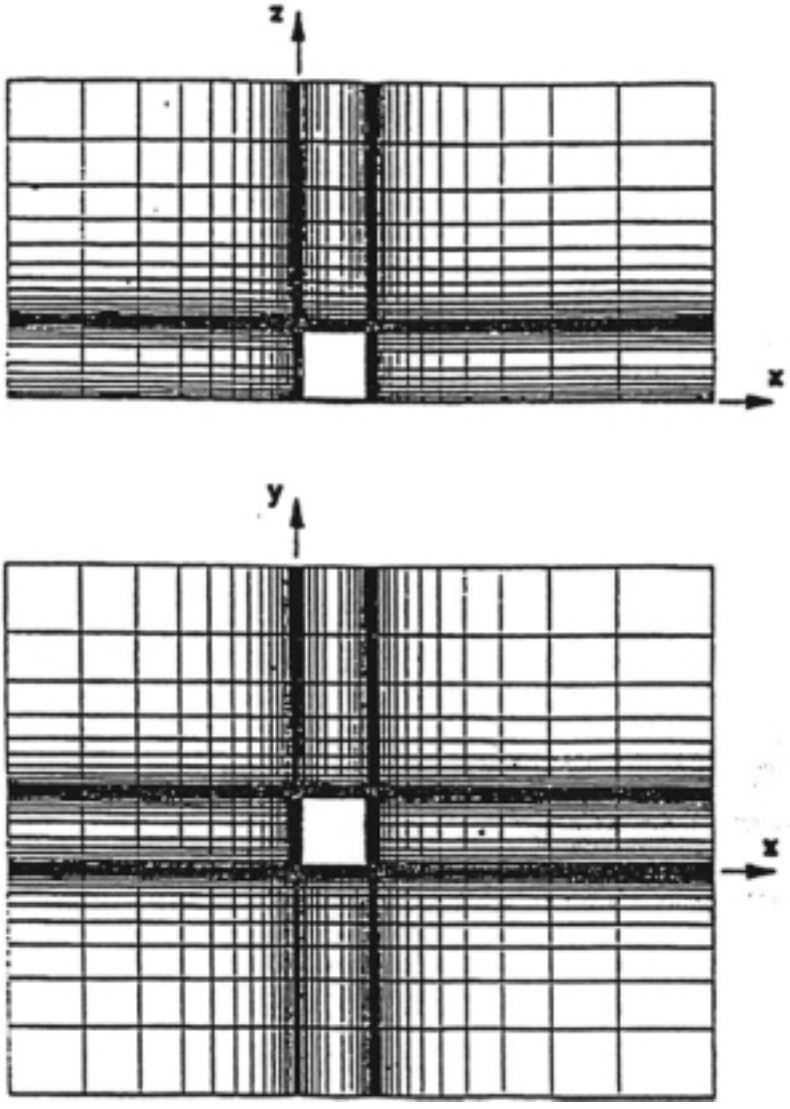

Figure 3.4. Example Profiles of Incident Flow Boundary Conditions. ***Zhou and Stathopoulos (1996).***

Computational domain extends to z 70 cm. Here, U is the velocity at height z, U_g **is** the velocity in the freestream, U_b is the velocity at the building height H, k and e (ε) are the kinetic energy and energy dissipation rate**.**

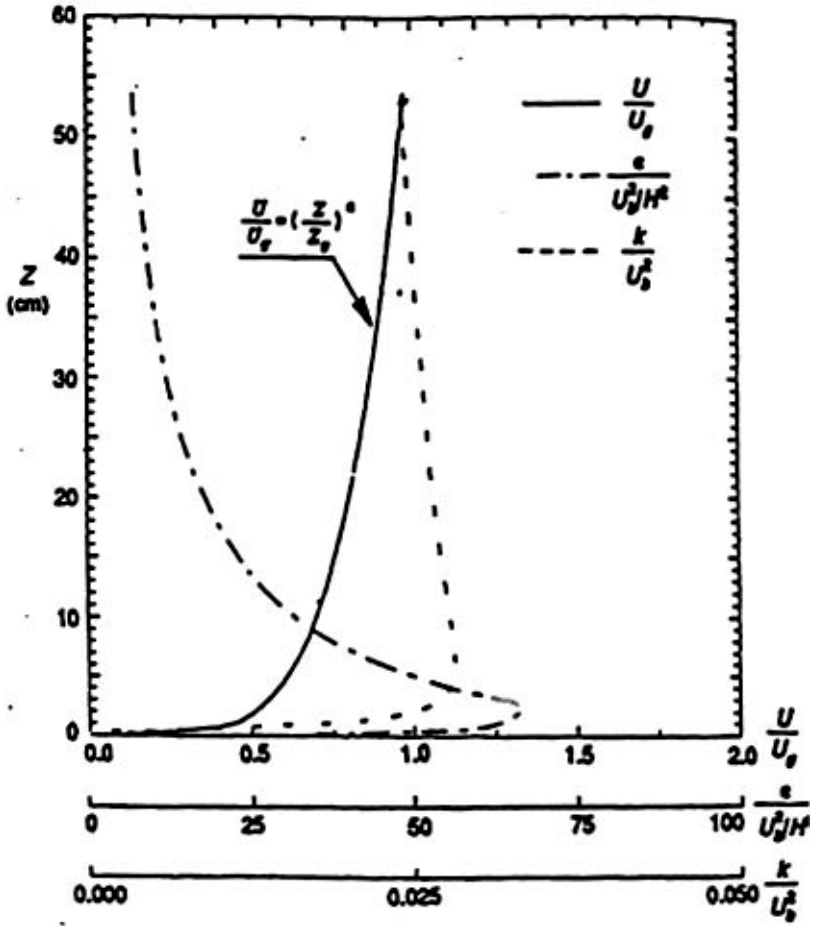

Figure 3.5. Computed Shapes of Rain drops of Various Equivalent Diameters. *Beard and Chuang (1987).*

Computation based on a balance between hydrostatic pressure, aerodynamic pressure, and surface tension forces.

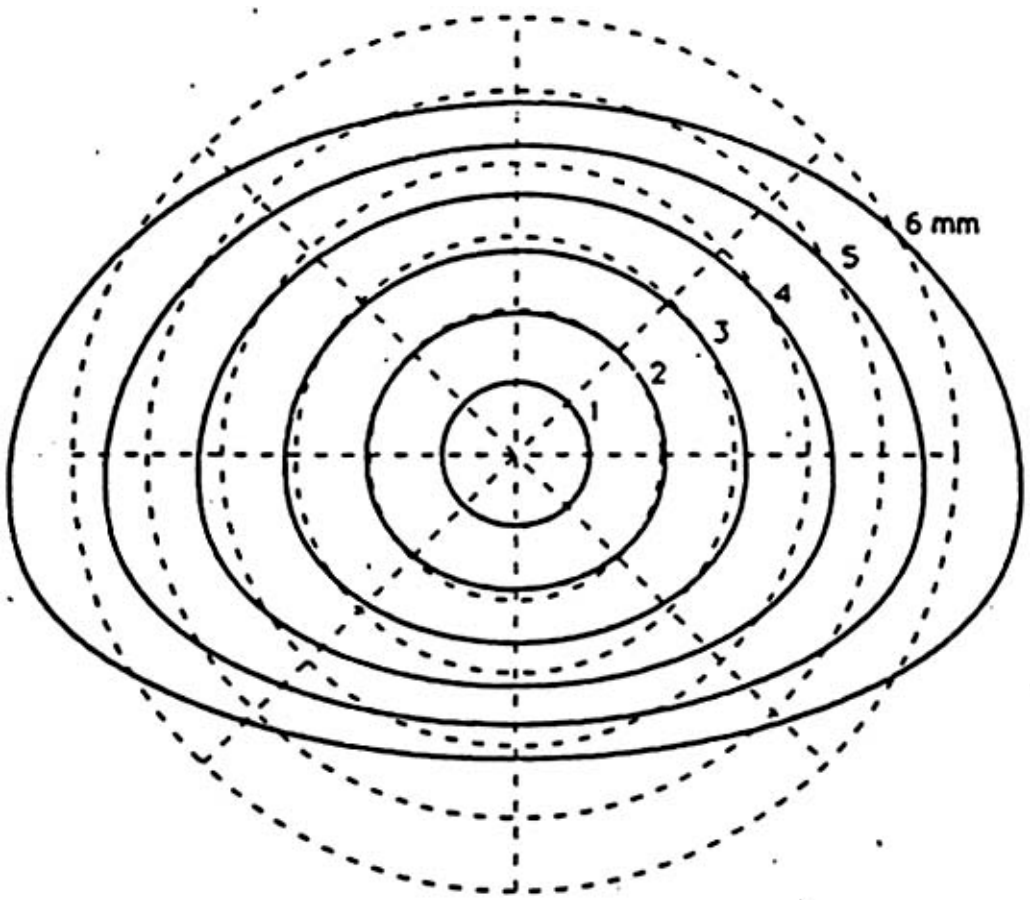

Figure 3.6. Equilibrium Drop Size Distribution as a Function of Drop Diameter. ***Brown and Whittlesey (1992).***

Calculated from a numerical simulation with 34 size bins.

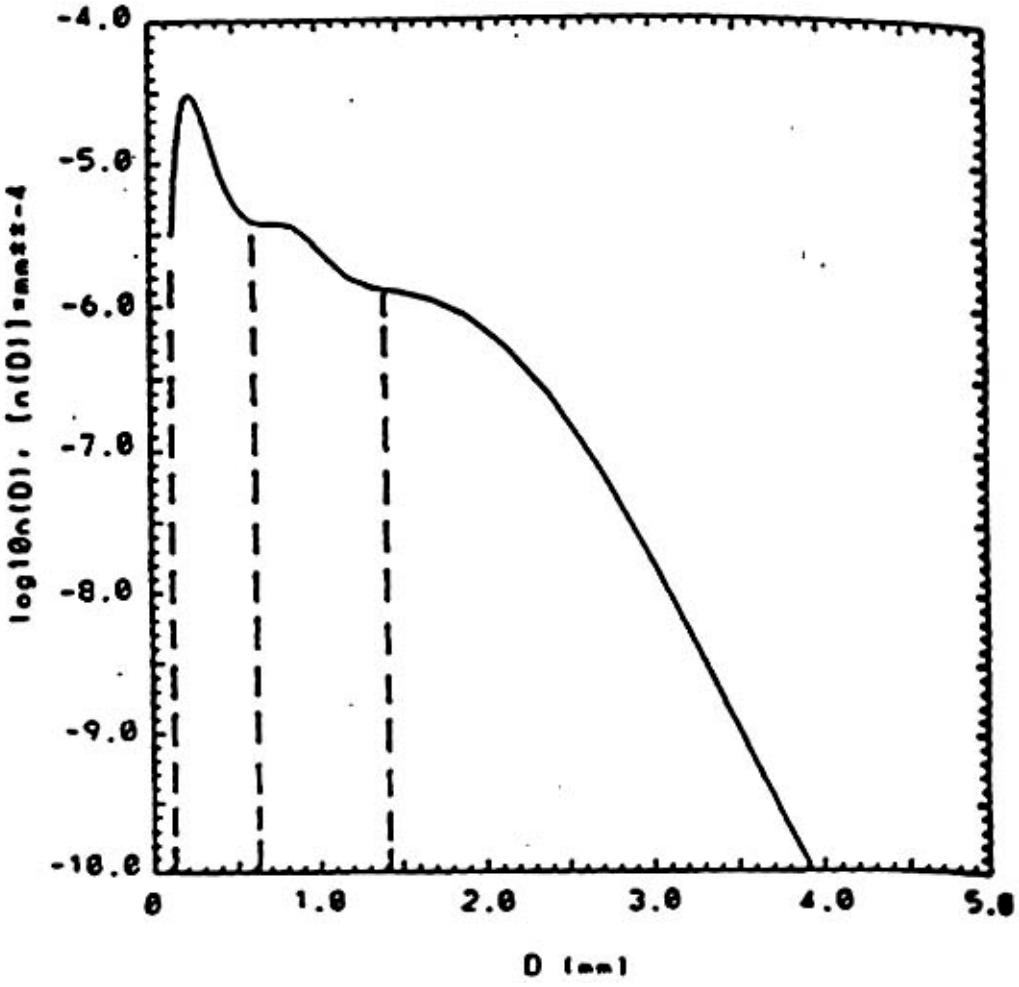

Figure 3.7. Schematic of a Disdrometer. ***Loffler-Mang et al. 1996.***

Signal processor not shown.

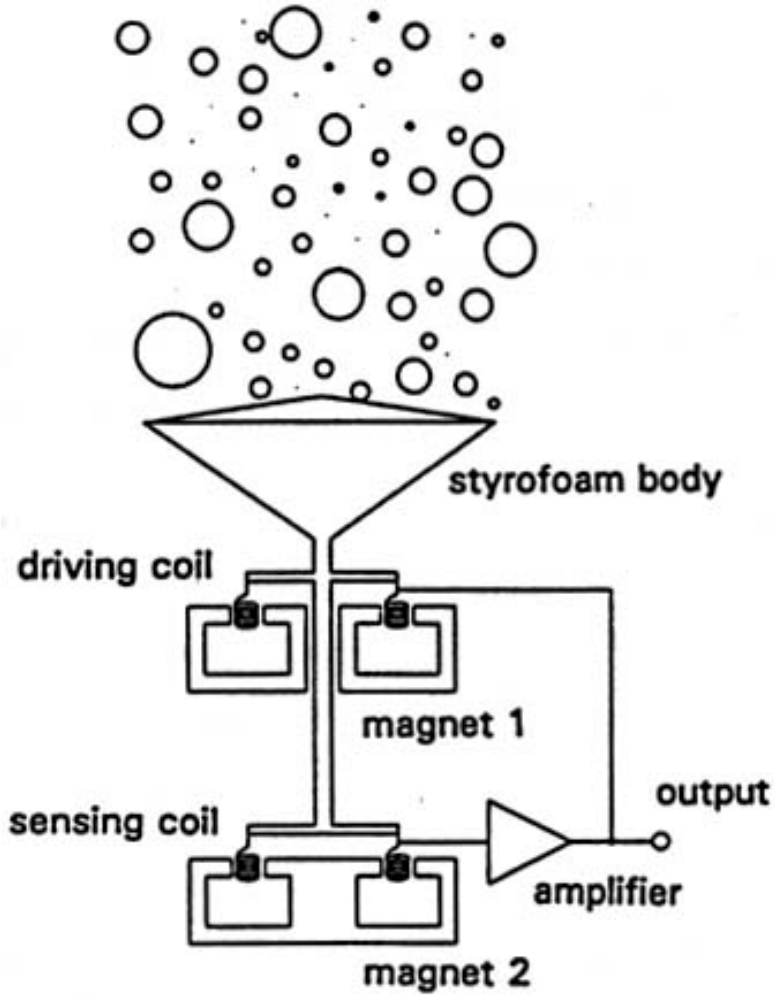

CHAPTER 4: REPORT SUMMARY

This project has focused on obtaining a better understanding of chemical and physical processes that further the deterioration of calcareous stone buildings. Investigation of such processes has occurred primarily at the 42-story Cathedral of Learning. However, some of the results obtained at the Cathedral can be extended to other limestone buildings in similar environments. Such information can aid conservators in assessing mechanisms of damage or in deciding on appropriate treatments for deteriorating buildings.

This report summarizes work conducted on the Cathedral of Learning project during November 15, 1996 and November 15. 1997. Specifically, we have reported on the status of two on-going research efforts. First, we described experiments at the Cathedral where particles were collected on air sampling filters as well as surrogate surfaces for vertical deposition. These samples were obtained during spring and summer 1996 as part of a larger study in which vertical gradients of pollutant concentrations and deposition fluxes were measured (Etyemezian et al., 1997; Appendix A). Scanning electron microscopy analysis on a limited number of samples suggests the presence of at least three types of particles, 1) calcium, sulfur, and silicon rich (Ca-S-Si), 2), aluminum, silicon, and iron rich (Al-Si-Fe), and 3) calcium and magnesium rich (Ca-Mg). Preliminary results also indicate that size distributions of particles found on air filters are different from those found on surrogate surfaces.

Second, we have described the development of two models: A computer model for describing airflow around the Cathedral, and a simple mathematical model for calculating trajectories of individual raindrops. The airflow model will utilize commercially available computational fluid dynamics software. Initially, the model will be used with basic building shapes such as cubes and rectangles. Results with these shapes will be compared with field and wind tunnel data from the literature. In later studies, we will use building shapes that better represent the geometry of the Cathedral. The airflow model will provide input parameters for other modeling efforts including the calculation of raindrop trajectories near the Cathedral..

REFERENCES

Alusa, AL. . 1975. The Role of Drop Breakup in the Development of Rain drop Size Distributions. Journal de Recherches Atmosphericues 9 (1):1-10.

Amoroso, G.G., and V. Fassina 1983. Stone Decay and Conservation: Atmospheric Pollution, Cleaning, Consolidation and Protection, *Materials Science Monographs* 11, Elsevier, 1983.

Beard, K.V., and C. Chuang. 1987. A New Model for the Equilibrium Shape of Rain drops. Journal of the Atmospheric Sciences 44 (11): 1509-1524.

Bock, E., and W. Sand. 1993. The Microbiology of Masonry Biodeterioration Journal of Applied Bacteriology 74: 503-514.

Brown, P.S. Jr., and S.N. Whittlesey. 1992. Multiple Equilibrium Solutions in Bleck-Type Models of Drop Coalescence and Breakup. Journal of Atmospheric Sciences 49 (23): 2319-2324.

Camuffo, D., M. Del Monte, C. Sabbioni, and O. Vittori. 1982. Wetting, Deterioration and Visual Features of Stone Surfaces in an Urban Area. Atmospheric Environment 16(9): 2253-2259.

Castro, I.P., and A.G. Robins. 1977. The Flow around a Surface-Mounted Cube in Uniform and Turbulent Streams. Journal of Fluid Mechanics 79 (2): 307-335.

Cermak, J.E., 1976. Aerodynamics of Buildings. In Annual Review of Fluid Mechanics 8: 75-106. Annual Reviews, Inc. Palo Alto, CA. 1976.

Choi, E.C.C.1993. Simulation of Wind-Driven Rain around a Building. Journal of Wind Engineering and Industrial Aerodynamics 46: 721-729.

Corke, T.C., and H.M. Nagib. 1976. As Cited in Hosker (1984). Sensitivity of Flow around and Pressures on a Building Model to Changes in Simulated Atmospheric Surface Layer Characteristics. lIT Fluids and Heat Transfer Report R76-1, May, Illinois Institute of Technology, Mechanics and Mechanical and Aerospace Engineering Deaprtment, Chicago, Illinois.

Davidson, C.I., and V.L. Wu. 1990. Dry Deposition of Particles and Vapors. *Chapter* 3 in *Acid Precipitation, Volume 2. Sources, Emissions, and Modeling,* D.C. Adriano ed., Advances in Environmental Sciences Series, Springer-Verlag, New York.

Deardorff, J.W.. 1969. A Numerical Study of Three-Dimensional Turbulent Flow at Large Reynolds Numbers Journal of Fluid Mechanics 41 (2): 453-480.

Del Monte, M., C. Sabbioni, and O. Vittori. 1981, Airborne Carbon Particles and Marble Deterioration, Atmospheric Environmentl5: 645-652.

Etyemezian, V., C.I. Davidson, S. Finger et al. 1995. Influence of Atmospheric Pollutants on Soiling of a Limestone Building Surface Progress Report for the NatiOnal Park Service. September, 1995.

Etyemezian, V., C.I. Davidson, S. Finger et al. 1996. Vertical Gradients of Pollutant Concentrations and Deposition Fluxes at the Cathedral of Learning. Progress Report for the National Park Service. November, 1996.

Etyemezian, V E., C.I. Davidson, S. Finger, M. Striegel, N. Barabas, and J. Chow 1997. Vertical Gradients of Pollutant Concentrations and Deposition Fluxes on a Tall Limestone Building. Submitted to the *Journal of the American Institute for Conservation,* November 1997.

Flagan, R.C., and J. H. Seinfeld. 1988. *Fundamentals of Air Pollution Engineering.* Prentice-Hall, New Jersey.

Freemantle, M. 1996. Historic Monuments Pose Challenge to Conservation Scientists Chemical and Engineering News 74: 20-23.

Friedlander, S.K. 1977. *Smoke, Dust, and Haze- Fundamentals of Aerosol Behavior,* Wiley, *New* York.

Gillespie. J.R., and R. List. 1978/1979. As cited in Brown and Whittlesey (1992). Effects of Collision-Induced Breakup on Dropsize Distributions in Steady-State Rain-Shafts. Pure Applied Geophysics 117: 599 –626.

Good, M.C., and P.N. Joubert. 1968. The Form Drag of Two-Dimensional Bluff-Plates Immersed in Turbulent Boundary Layers. Journal of Fluid Mechanics 31 (3): 547-582.

Hamilton, R.J., and T.A. Mansfield. 1993. The Soiling of Materials in the Ambient Atmosphere. Atmospheric Environment 27a (8): 1369-1374.

Hosker, R.P.Jr., 1979. As cited in Hosker (1984). Empirical Estimation of Wake Cavity Size Behind Block-Type Structures. In *Preprints of Fourth Symposium or Turbulence, Diffusion, and Air Pollution,* Rena, Nevada. January, pp 603-609, American Meteorological Society, Boston, MA, 1979.

Hosker, R.P.Jr., 1984. Flow and Diffusion near Obstacles In: *Atmospheric Science and Power Production* Report for United States Department of Energy. Darryl Randerson, editor.

Hutchinson, A.J., J.B.Johnson, G.E.Thompson, G.C. Wood, P.W. Sage, and M.J. Cooke. 1992. The Role of Fly-ash Particulate Material and Oxide Catalysts in Stone Degradation. Atmospheric Environment 26a: 2795-2803.

King, W.D., and S.Dujmovic. 1987. Fluid Flow and Particle Trajectories around Simple Bodies: Impaction of Snowflakes on Car Windshields. American Journal of Physics 55(2): 149-154.

Lakehal, D., P.G. Mestayer, J.B. Edson, S. Anquetin and J.F. Sini. 1995. Eulero-Lagrangian Simulation of Rain drop Trajectories and Impacts within the Urban Canopy Atmospheric Environment 29: 3501-3517.

Lam, C.K.G., and K. Bremhorst. 1981. A Modified Form of the K-ε Model for Predicting Wall Turbulence. Journal of Fluids Engineering 103: 456-460.

Launder, B.E., and D.B. Spalding. 1972. *Lectures in Mathematical Models of Turbulence.* Academic Press London, England.

Launder, B.E., and D.B. Spalding. 1974. The Numerical Calculation of Turbulent Flows. Computer Methods in Applied Mechanics and Engineering 3: 269-289.

Loffler-Mang, M., K.D. Beheng,, and H.G. Karlruhe. 1996. Drop Size Distribution Measurements in Rain-a Comparison of Two Sizing Methods. Meteorol. Zeitschrift 5: 139-144.

McGee, E.S. 1997. Surficial Alteration at the Cathedral of Learning in Pittsburgh, Pennsylvania. USGS Open-File Report 97-275.

Mikkelsen, A.C., and F.M. Livesey. 1995. Evaluation of the Use of the Numerical K-ε Model Kameleon II, for Predicting Wind Pressures an Building Surfaces. Journal of Wind Engineering and Industrial Aerodynamics 57: 375-389.

Minson A.J., C.J. Wood, and R.E. Belcher. 1995. Experimental Velocity Measurements for CFD Validation. Journal of Wind Engineering and Industrial Aerodynamics 58: 205-215.

Mossotti, V.G., and A.R. Eldeeb. 1994. Calcareous Stone Dissolution by Acid Rain. Manuscript in progress. Version-0 7, Dec. 12, 1994.

Murakami, S., and A. Mochida. 1989. Three-Dimensional Numerical Simulation of Turbulent Flow around Buildings Using the k- ε Model. Building and Environment 24(1): 51-64.

Murakami, S., A. Mochida, R. Ooka. S. Kato, and S. Iizuka. 1996. Numerical Prediction of Flow around a Building with Various Turbulence Models Caomparison of k- ε EVM, ASM, DSM, and LES with Wind Tunnel Tests. ASHRAE Transactions 102(1): 741-753.

Neff, D.E., and R.N. Meroney. 1996. Reynolds Number Independence of the Wind Tunnel Simulation of Transport and Dispersion about Buildings. Unpublished Report 23 pages. 15 references.

Nord, A.G., A. Svardh, and K. Tronner. 1994. Air Pollution Levels Reflected in Deposits on Building Stone. Atmospheric Environment 28(16): 2615-2622.

Ogawa, Y. and S. Oikawa. 1982. A Field Investigation of the Flow and Diffusion around a Model Cube. Atmospheric Environment 16: 207-222.

Ogawa, Y. S. Oikawa, and K. Uehara. 1983a. Field and Wind Tunnel Study of the Flow and Diffusion around a Model Cube-II. Nearfield and Cube Surface Flow and Concentration Patterns. Atmospheric Environment 17: 1161-1171.

Ogawa, V., S. Oikawa, and K. Uehara. 1983b. Field and Wind Tunnel Study of the Flow and Diffusion around a Model Cube-I. Flow Measurements. Atmospheric Environment 17: 1145-1159.

Paterson, D.A., and C.J. Apelt. 1989. Simulation of Wind Flow around Three-Dimensional Buildings. Building and Environment 24(1): 39-50.

Plate, E., 1982. Wind Tunnel Modelling of Wind Effects in Engineering. In: *Engineering Meteorology vol I.* E.Plate, editor, Elsevier, Amsterdam, Oxford, and New York. 573-640.

Ramaswamy, V., and P. Chylek. 1979. Shape of Rain drops. In Proceedings of the International Workshop on Light Scattering by Irregularly Shaped Particles. June, 1979. 334 pages. pp 55-61. Plenum, Albany, New York. 1979.

Riezebos, H.T., and G.F. Epema. 1985. Drop Shape and Erosivity Part II: Splash Detachment, Transport, and Erosivity Indices. Earth Surface Processes and Landforms 10: 69-74.

Robins. A.G., and I.P. Castro. 1977a. A Wind Tunnel Investigation of Plume Dispersion in the Vicinity of a Surface Mounted Cube-II. The Concentration Field. Atmospheric Environment 11: 299-311.

Robins, A.G., and I.P. Castro. 1977b. A Wind Tunnel Investigation of Plume Dispersion in the Vicinity of a Surface Mounted Cube-I. The Flow Field. Atmospheric Environment 11: 291-297.

Saathoff, P.J., T. Stathopoulos, and M. Dobrescu. 1995. Effects of Model Scale in Estimating Pollutant Dispersion near Buildings. Journal of Wind Engineering and Industrial Aerodynamics 54: 549-559.

Sabbioni, C. 1994. Effects of Air Pollution on Historic Buildings and Monuments Scientific Basis for Conservation Physical, Chemical, and Biological Weathering. European Cultural Heritage Newsletter on Research 8 (1): 2-6.

Schlichting, H., 1960. *Boundary Layer Theory, 4th ed.,* McGraw Hill, New York, London, and Paris.

Scholes, A.J., and I.H.Johnson. 1995. Impact of CFD Techniques on Environmental Engineering Environmental Engineering 8 (2): 12-17.

Schwoeble, A.J., H.P.Lentz, W.J. Mershon, and G.S. Casuccio. 1990. Microimagining and Off-line Microscopy of Fine Particles and Inclusions. Materials Science and Engineering a124: 49-54.

Seinfeld, J.H. 1986. *Atmospheric Chemistry and Physics of Air Pollution* John Wiley and Sons, New York.

Selvam, R.P. 1996. Numerical Simulation of Flow and Pressure around a Building ASHRAE Transactions 102(1): 765-772.

Snyder, W.H., and R.E. Lawson Jr. 1976. Determination of a Necessary Stack Height for a Stack Close to a Building. A Wind Tunnel Study. Atmospheric Environment 10: 683-691.

Twohy, C.H., and D. Rogers. 1993. Airflow and Water-Drop Trajectories at Instrument Sampling Points around the Beechcraft King Air and Lockheed Electra. Journal of AtmosDheric and Oceanic Technology 10: 566-578.

Wilmzig, M., and E. Bock 1995. Endangerment of Mortars by Nitrifiers, Heterotrophic Bacteria and Fungi. In *Biodeterioration and Biodegradation* 9 eds. A Bousher et al., Institution of Chemical Engineers, Rugby, UK, 195-197.

Young, P. 1996b. Mouldering Monuments. New Scientist 152: 37-38.

Zhou, Y., and T. Stathopoulos. 1996. Application of Two-Layer Methods for the Evaluation of Wind Effects on a Cubic Building. ASHRAE Transactions 102(1): 754-764.

APPENDIX A: VERTICAL GRADIENTS OF POLLUTANT CONCENTRATIONS AND DEPOSITION FLUXES TO A TALL LIMESTONE BUILDING. MANUSCRIPT SUBMITTED TO JAIC ON NOVEMBER 11, 1997.

Vertical Gradients of Pollutant Concentrations and Deposition Fluxes on a Tall Limestone Building

V. Etyemezian[1*], C.I. Davidson[1] , S. Finger[1], M. Striegel[2], N. Barabas[3], and J. Chow[4]

[*]Corresponding Author

[1]Deptartment of Civil and Environmental Engineering
Carnegie Mellon University
Pittsburgh, PA 15213

[2]NationaI Center for Preservation Technology and Training
NSU Box 5682
Natchitoches, LA 71497

[3]Department of Civil and Environmental Engineering
University of Michigan
116 EWRE Building
1351 Beat Avenue
Ann Arbor. MI 48109

[4]Desert Research Institute
5625 Fox Avenue
P.O. Box 60220
Reno, NV 89506

Submitted to the Journal of the American Institute for Conservation

11/10/97

1. ABSTRACT

The role of air pollutants in the soiling of a limestone building was investigated by measuring pollutant airborne concentrations and deposition at different heights at the Cathedral of Learning in Pittsburgh, Pennsylvania. Airborne concentrations of SO_4^{2-} particles, carbon particles, SO_2 gas, and total NO_3 (particles + HNO_3) were measured simultaneously on the fifth floor, sixteenth floor, and roof (forty-second floor), while laser particle counts of>0.5 μm and >5 μm particles were obtained on the fifth and sixteenth floors. SO_2 deposition fluxes to wall-mounted surrogate surfaces were measured at a total of nine locations on the fifth and sixteenth floors. Measurements were conducted during four time periods over the course of one year, each time period lasting four weeks. Results showed that airborne concentrations of the chemical species were invariant with height. Airborne number concentrations of>0.5 μm particles corroborated this result. Although not reflected in the chemical data, measured number concentrations of>5 μm particles on the sixteenth floor were on average 30% greater than those on the fifth floor. The spatially averaged highest and lowest deposition velocities of SO_2 (1.0 cm/s and 0.6 cm/s) never differed by more than a factor of two for the different time periods. The relative differences in deposition velocities from one location to another were consistent throughout all of the sampling experiments. Sixteenth floor deposition velocities were greater than those on the fifth floor but this was due, at least in part, to the fact that sampling locations on the sixteenth floor were more exposed to wind. The absence of gradients suggests that soiling patterns on the Cathedral are determined by the competing processes of pollutant deposition and rain washing. This hypothesis is supported by comparing soiling patterns on the Cathedral from the 1930's with recent patterns: Archival photographs show much greater amounts of soiling, consistent with the greater air pollution levels that existed then. Results of this study can assist in designing cleaning and treatment protocols for other buildings with similar geometry in similar environments.

2. INTRODUCTION

Several types of building stone deterioration have been well documented, including discoloration, erosion of material, and changes in the physical and chemical characteristics of the surface. Developing strategies to prevent this deterioration requires knowledge of the processes by which the damage occurs, for example

by deposition of air pollutants or by biological growth on the stone surface. Furthermore, the choice of cleaning and restoration techniques depends on the processes causing the damage.

Differentiation between pollutant deposition and biological growth is difficult and generally requires on-site testing. Unfortunately, getting access to the building walls sometimes demands scaffolding, and due to expense scaffolds are typically not erected until shortly before restoration work begins Thus, early identification of the primary deteriorating or discoloring agents is oflen difficult and tentative.

In this study, field measurements of air pollutant concentrations and deposition are used in conjunction with archival photographs to draw conclusions regarding the role of pollutants in the soiling of a tall building. The structure of interest is the 42-story Cathedral of Learning, a National Historic Landmark on the University of Pittsburgh campus (Figure 1). The building is made of Indiana limestone and was constructed between 1929 and 1937 Since the time of construction, there have been numerous air pollution sources within a few kilometers of the building. These include steel manufacturing plants that employ coke ovens and blast furnaces, a coal-burning steam plant, heavy motor vehicle traffic, coal-burning railroads and riverboats, and a large number of domestic coal combustion sources such as home furnaces

At present, two sides of the Cathedral of Learning have extensive soiling, particularly on the lower two-thirds of the building In a study on the alteration crust at the Cathedral, McGee (1995; 1997) reports that Fe-, Si-. and Al- rich fly ash particles are found in samples of soiled surfaces and that such particles are much less prevalent in samples of unsoiled surfaces. This result indicates that surface soiling at the Cathedral is primarily due to deposition of anthropogenic particles to the building walls.

This research had three major objectives. First, we wanted to identify the extent to which airborne concentrations of certain pollutants vary with height on the Cathedral. The pollutants of interest include SO_4^{2-} particles, carbon particles. SO_2 gas, total NO_3^- (HNO_3 gas and NO_3^- particles), and total particle number. Such information can provide insight on the relative importance of local and regional sources of pollutants as well as pathways for delivery of pollutants to the building surface. Second, we wished to examine variations in dry deposition of SO_2 with height and location. This can provide information on whether the variability in pollutant deposition is partly responsible for the observed soiling patterns. Third, we wished to consider long-term variations in soiling patterns on the building in light of changes in pollution concentrations. This part of the project made use of previously obtained historical pollutant data

as well as archival photographs. Such information enabled us to investigate the roles of pollutant deposition and subsequent washoff by rain in affecting the soiling. Although this study focused on only one building, the results may also be applicable to geometrically similar buildings in similar environments.

3. BACKGROUND

Calcareous stones exposed to the atmosphere are vulnerable to attack by several processes which occur naturally. These processes include microbial activity on the stone surface, dissolution by rain, and physical stresses such as freeze-thaw cycles. Anthropogenic air pollutants are frequently responsible for accelerated deterioration, both directly through physical and chemical attack, and indirectly by providing substrates for microbial growth.

In recent years,considerable attention has been given to the role of biological agents in damage to buildings (e.g. Young. 1996a: Freemantle, 1996. Wilmzig and Bock. 1995*:* Mitchell et al. 1996). In general, species of fungi, algae, lichens, and bacteria have been found on surfaces of building stones (Bock and Sand. 1993). These organisms can accelerate deterioration either by physical processes such as alteration of the normal wetting-drying cycle (Young. l996b), or by chemical processes such as mineral and organic acid production and secretion of metal-chelating agents (Palmer et al., 1991). It is difficult to estimate the quantities and overall effects of biodeteriogens, in part because the fecundity and productivity of these organisms is strongly dependent on microenvironmental factors. These include insolation, stone type and porosity, surface and air temperatures, availability of a suitable substrate, and availability of water from incident rain, stone pore capillarity, or condensation and evaporation cycles (Bock and Sand. 1993). In addition to the expected temporal variability caused by changes in the weather (Tayler and May, 1991), there can be considerable spatial variability over short distance scales Understanding biodeterioration processes is further confounded by a possible correlation between air pollution levels and biodeterioration rates (Young, 1996b). For example, Warscheid et al (1991) have shown that some chemo-organotrophic bacteria isolated from sandstones of historic monuments are able to utilize petroleum derivatives as sources of carbon as well as energy.

Several categories of air pollutants can accelerate the natural deterioration of Stone through two primary processes, wet and dry deposition (e.g. Sherwood et al., 1990, Anioroso and Fassina, 1933). The former refers to the deposition of a pollutant by a precipitation process such as rain or snow; acid rain is an example. Several authors have considered the effects of acid rain on calcareous stones (Winkler, 1996; Braun and Wilson, 1970; Mossotti and Eldeeb, 1994; Livingston, 1992; Hutchinson et at., 1993). Dry deposition includes those process by which pollutants are transported to the surface in the absence of precipitation and become physically or chemically bound to the surface. Damage to calcareous building stone by dry deposition has been attributed largely to sulfur dioxide gas (SO_2). For example, Meierding (1993) found that mean surface recession rates of century-old Vermont marble tombstones in the United States were well correlated with SO_2 concentrations. In addition, some authors point out that nitric acid gas (HNO_3) may also be sorbed onto a carbonate surface (Kirkitsos and Sikiotis, 1995; Fenter et al., 1995).

The removal of SO_2 by certain stone twes is a well-documented phenomenon (Judeikis et al 1978). Calcareous stones subjected to high relative humidity develop a moist surface layer where SO_2 can readily dissolve (Spiker et al., 1995; Spedding, 1969); in general, the rate of dissolution increases at higher relative humidities and wind speeds (Spiker et al., 1995). Dissolved SO_2 can then oxidize to form a sulfite (SO_3^{2-}) or sulfate (SO_4^{2-}) species. The oxidation process results in the production of acid which can cause the calcium carbonate ($CaCO_3$) in the stone to dissolve. When calcium ions (Ca^{2+}) combine with SO_3^{2-} or SO_4^{2-}, CO_3^{2-} is effectively displaced from the stone surface. This process, known as sulfation, may also involve gaseous and particulate air pollutants other than sulfur species. Gases such as ozone (O_3) (Haneefet al., 1992) and nitrogen dioxide (NO_2) (Johansson et al., 1988) have been shown to increase SO_2 deposition to limestone. Surface crust analyses of damaged stone have also shown a close relation between deposited anthropogenic particles and the formation of gypsum crystals (Zappia, 1993*;* Sabbioni, 1994*;* Del Monte et al., 1981), suggesting a relationship between sulfation and the presence of airborne particles. However. Hutchinson et al. (1992) have reported that limestone seeded with coal fly ash or transition metal oxide catalysts is not susceptible to elevated SO_2 deposition. These authors suggest that seeding stone samples with oxidation catalysts has a negligible effect because natural stones already contain high levels of impurities. In contrast, seeding pure $CaCO_3$ with metal oxide catalysts does increase the rate of sulfation.

Urban air pollution studies have considered effects of buildings on dispersion of vehicle emissions as well as dispersion of individual plumes from stationary sources. In general, dispersion of vehicle emissions in street canyons is a function of the building height divided by the street width, known as the aspect ratio (Lee and Park, 1994), as well as the geometric configurations of city blocks, the ambient wind direction, and the movement of motor vehicles (DePaul and Sheih, 1985; Dabbert and Hoydysh, 1991; Hoydysh and Dabbert, 1994). Qin and Chan (1993) and Qin and Kot (1993) have reported that significant differences in carbon monoxide and nitrogen oxides (NO_x) concentrations exist between the top and bottom of buildings surrounding Street canyons in Guangzhou. China Qin and Kot (1990) have also shown that vehicle traffic near a 31 Story (100 m) tower can result in elevated NO_x concentrations near the downwind building surface up to a height of 66 meters. The effect of a building on the dispersion of a stationary source plume is, in general, dependent on the building geometry, source location, and prevailing wind conditions (e.g. Lee Ct al., 1991; Huber et al., 1991; Thompson. 1993). In some eases, direct measurement of the spatial variability of surface concentrations may be easier than application of theoretical considerations.

4. EXPERIMENTAL

Vertical gradients of pollutant concentrations and deposition fluxes were measured by sampling at varying elevations on the Cathedral of Learning. Three locations were chosen for sampling: the fifth floor and sixteenth floor patios on the southeastern façade and the patio on the roof (Figure 2). The southeastern façade was chosen for two reasons. First, it was one of the two heavily soiled sides of the building (the northeastern façade being the other). Second, the fifth floor and sixteenth floor patios on the southeastern façade were frequently on the windward side of the Cathedral (Figure 3) where mixing is not affected by the wake cavity of the building.

The vertical gradient experiments were conducted on four separate occasions from the period of 11/20/95 to 8/21/96. The experiments were scheduled so that representative sets of data were obtained during the different seasons of the year (Table 1). Each set of experiments included four consecutive sampling periods of one week each. Sampling was uninterrupted throughout this period except for

approximately three hours each week for changing samples. Airborne concentrations of SO_4^{2-} particles, SO_2 gas, and total NO_3^- species (NO_3^- particles and HNO_3 gas) were measured. Airborne concentrations of elemental and organic carbon particles were measured during the fall and winter experiments only. For the spring and summer experiments, polycarbonate membrane filters were used in place of the carbon measurements to obtain samples for scanning electron microscopy analysis (SEM). Laser particle counters were used to provide real-time data for number concentrations of particles with diameter> 0.5 μm and> 5 μm. Each set of experiments also included two two-week measurements of SO_2 deposition fluxes.

All sampling was conducted using identical sets of sampling equipment at each site, two replicate sets for airborne concentrations and four sets for deposition fluxes. Airborne concentrations were measured on patios on the fifth floor, sixteenth floor, and roof of the Cathedral Deposition flux and laser particle counter measurements were conducted on the fifth and sixteenth floors only.

4a. *Airborne Concentrations of Chemical Species*

Many of the procedures for measuring concentrations at the Cathedral were developed by Gould et al. (1993). Air samplers were placed on supports 1.5 m above the surface of the patios. Concentrations of anions were measured using multistage Teflon filterpacks (Savillex Corporation) with 47 mm diameter filters. Each filterpack included a Teflon Zefluor filter (Gelman P5PL047, 1 μm pore size) followed by two back-to-back nylon Nylasorb filters (Gelman 66509). These were followed by two sets of potassium carbonate impregnated cellulose filters (Whatrnan 1441-047, ashless), with each set consisting of two back-to-back filters. The Teflon filters were used to sample SO_4^{2-} and NO_3^- particles, while the nylon and cellulose filters were used to sample HNO_3 and SO_2, respectively. A critical flow orifice maintained the flow at 1 liter per minute.

Stainless steel filter holders (Millipore XX50-047-10. open-faced) were used with 47 mm diameter quartz fiber filters (Pallflex 2500 QAT-UP) to measure carbon. A critical flow orifice maintained the flow at 3 liters per minute. These same filter holders were used with polycarbonate membrane filters (Costar Nuclepore PC-MB-47mm. 0.4 μm pore size) for SEM analysis. A metering valve (Hoke 1656 G4YA) was used to maintain the flow at 0.2 liters per minute through the membrane filters For all filter

sampling systems, a dry test meter (Singer DTM- 115) was used to obtain accurate flow rates at the beginning and end of each sampling run.

The Teflon, nylon, quartz. and polycarbonate filters were used as received from the manufacturer without washing. The cellulose filters were immersed in a solution consisting of 76 ml deionized (DI) water, 24 ml glycerin, and 15 g K_2CO_3. The filters were then dried on a hot plate covered with clean aluminum foil. Dry filters were placed in clean polyethylene bags (Clean Room Products 6 MIL-0406), heat sealed, and stored in a dessicator. One batch of cellulose filters was prepared at the beginning of each of the four sets of sampling experiments and used throughout that set.

Filterpacks and associated tubing were washed using three rinses with DI water, one rinse with methanol (Fisher Scientific, Optima grade), 30 minute sonication in a DI water bath, and two subsequent rinses with DI water. All procedures after washing such as drying, loading, assembling, and unloading of the filterpacks were performed inside a laminar flow hood. Filters were handled only with clean Teflon-coated tweezers. Assembled filterpacks were placed in clean polyethylene bags. Field blanks of all filters were prepared in an identical manner as the samples. Air was drawn through the blanks for 3-8 minutes prior to each sampling period.

When unloading the filterpacks, the same contamination control procedures were observed. The Teflon, nylon, and cellulose filters were placed in clean 30 ml polypropylene bottles. The two sets of back-to back cellulose filters were placed in separate bottles, and each set was analyzed individually. The quartz fiber and polycarbonate membrane filters were unloaded into clean 47 mm polypropylene petri dishes. With the exception of the polycarbonate membrane samples, all filters were frozen for later analysis. The quartz fiber filters were shipped frozen to the Desert Research Institute for analysis by the thermal optical reflectance method (Chowet al., 1993).

The Teflon, nylon, and cellulose filters were analyzed by ion chromatography. Extractions were performed in a laminar flow hood. The upstream faces of the Teflon filters were wetted with 1 ml methanol, and 29 ml of DI water were subsequently added to the sample bottle. Thirty ml of 0.003 M sodium hydroxide and 30 ml of 0.05% hydrogen peroxide were added to the bottles containing the nylon and cellulose filters, respectively. Sample bottles were sonicated for 45 minutes. After sonication, the nylon

and Teflon filters were removed from the sample bottles and discarded. The cellulose filters remained immersed in the extract solution. Extract solutions were refrigerated in order to maintain sample integrity.

Ion chromatography analysis was generally performed within two or three days of the extractions. Analyses were performed on a Dionex 4500i ion chromatograph using a 4mm AS4A anion column. Samples and standard solutions for calibrating the instrument were manually injected. After each injection, the syringe was rinsed with DI water several times. A standard solution was analyzed at least once every two hours. All sample handling occurred in a laminar flow hood.

4b. *Laser Particle Counters*

Two TSI model 3755 laser particle counters (LPC) were used in these experiments The LPCs were mounted with the nozzle side facing down at a height of 1 5 m above the patios. A laptop computer was used to log particle count data on a two minute basis. Some data were not properly logged during sampling periods either because the laptop did not record LPC signals, or due to clogging of the inlet with large particles. Problematic data were easily recognized and discarded. High particle concentrations measured by the LPC had to be corrected for double counts in accordance with the manufacturer's recommendations.

4c.*Vertical Deposition Sampling*

Deposition fluxes of SO_2 were measured on 125 mm potassium carbonate impregnated cellulose filters (Whatman 1441-125, ashless). Four of these filters were mounted on a thin Teflon-coated aluminum plate. Flat Teflon rings (inner diameter = 105 mm) were placed on top of the filters. Labeling tape was used to fasten the rings to the plate. The fully assembled plates were transported to the Cathedral in a polyethylene tray encased in a clean bag. Field blanks were exposed for approximately ten minutes in an identical manner as the samples. As With the airborne concentration filters, loading, unloading, and drying of equipment were performed on a clean surface in a laminar flow hood. Extraction and ion chromatography analyses were conducted in the same manner as for the airborne concentration cellulose filters except that 120 ml of hydrogen peroxide extraction solution was used for each filter.

Nine Teflon-coated aluminum plates were exposed simultaneously in each deposition sampling period. The samples were placed at six locations on the fifth floor (5a-5f) and three locations on the sixteenth floor (16a-16c) (Figure 2) Locations 5a-5d and 16b were in areas where visible soiling was present, while the remaining four were in areas that were free of soiling. To avoid exposure to rain, each Teflon-coated aluminum plate was placed under a galvanized aluminum rainshield (Figure 4). Locations 5b and 5c were adjacent and were placed under one larger rainshield. Previous work has shown that rainshields used in different configurations may affect SO_4^{2-} particle dry deposition (Davidson et al., 1985). The effect of the rainshields on SO_2 gas deposition was considered by comparing fluxes to the top two and bottom two deposition surfaces for all sampling locations. If the rainshield had interfered with SO_2 delivery, then deposition to the upper surfaces should have been different from deposition to the lower surfaces. The average fluxes to the top and bottom surfaces were not found to differ with statistical significance.

5. RESULTS

5a. Airborne Concentrations of Chemical Species

Airborne concentrations of SO_4^{2-} particles, elemental carbon particles, SO_2 gas. and total No_3^- are shown in Figures 5 and 6. Results of SEM analyses of the polycarbonate membrane filters will be presented in a subsequent paper. Averages and standard deviations of concentrations are based on the two side by side replicate samplers. When one of the replicate samplers malfunctioned, the concentration was obtained from a single sample. The standard deviation for a single sample is approximated by the concentration multiplied by the average coefficient of variation (COV) for all samples for which replicates are available (44 of 48 samples). The COV has been calculated as the standard deviation divided by the average concentration. Each sample has been blank-corrected by subtracting the average mass of analyte found on field blanks from the mass of analyte found on the sample (Table 2).

Several authors have documented artifacts associated with NO_3 species measurement using staged filterpack systems (Appel et al., 1981; Mulawa and Cadle, 1985; Hering et al., 1988). For example, volatile

NO_3^- aerosol deposited on Teflon filters may subsequently evaporate. The vapor then redeposits on the downstream nylon filters resulting in overestimated HNO_3 gas and underestimated NO_3 particle concentrations. In order to account for possible sampling artifacts, NO_3 species concentrations from the experiments reported here are conservatively expressed as total NO_3^- (HNO_3 gas and NO_3^- particles) by summing values from the Teflon and nylon filters.

SO_2 concentrations are based on the chemical analyses of both the nylon and cellulose filters, since the nylon filters tend to remove some SO_2 from the air stream (Chan et al., 1986; Cadle and Mulawa, 1987). Experiments in the fall of 1995 showed that two sets of cellulose filters may be needed to capture all of the SO_2 at high concentrations. Therefore, a second pair of cellulose filters was added downstream of the first set for the latter part of the fall experiments and all remaining runs.

As with the other airborne concentration data presented here, the standard deviations of elemental carbon concentrations reflect the variability between two side by side replicate airborne concentration samplers. However, only 10 of the 48 samples and 5 of the 19 field blanks have had replicate chemical analyses. Therefore, the standard deviations of carbon mass on each filter are approximated by the average COV of the samples for which replicate chemical analyses have been performed.

5b. *Laser Particle Counts*

Examples of particle counts for the period 2/16/96-2/20/96 appear in Figure 7. Although particle concentration data are available on a two-minute average basis, the concentrations in Figure 7 have been averaged over ten minutes to improve legibility. Daily average, maximum, and minimum particle concentrations are plotted in Figure 8 and weekday vs weekend particle concentrations are presented in Table 3.

5c. *Vertical Deposition Flux and Vertical Deposition Velocity*

Measured vertical deposition fluxes and deposition velocities appear in Figures 9 and 10. SO_2 flux averages and standard deviations are based on the four replicate cellulose filters on each Teflon-coated aluminum

plate. Vertical deposition flux is a measure of how much SO_2 has deposited onto the surrogate surface per unit area per unit time. The deposition velocity V_d is calculated by dividing the deposition flux by the airborne concentration. The average deposition velocity and standard deviation have been calculated using:

$$V_d = 0.0116 \bullet F/C$$

$$\sigma_v = \sqrt{\left(\frac{0.0116 \bullet \sigma_F}{C}\right)^2 + \left(\frac{0.0116 \bullet F \bullet \sigma_C}{C^2}\right)^2}$$

where

V_d = deposition velocity, cm/s.

F = average flux to surrogate surfaces. ng/(cm^2 • day).

C = average airborne concentration, $\mu g/m^3$.

σ_υ = standard deviation of deposition velocity. cm/s.

σ_F = standard deviation of deposition flux. ng/(cm^2 • day).

σC = standard deviation of airborne concentration, $\mu g/m^3$,

and 0.0116 is a conversion factor

The average airborne concentration C used for calculating V_d on either the fifth or sixteenth floor is based on the two one-week airborne concentrations measured on the corresponding floor. It is assumed that this average airborne concentration applies to all of the flux measurement sites on that patio. This is a reasonable assumption based on the agreement between the two replicate sets of filters sampled on each patio.

The surrogate surfaces used in this study are considered to be perfect sinks for SO_2, and thus SO_2 is assumed to be instantaneously and completely removed when it reaches the filter. The deposition velocity is thus only a measure of gas phase mass transport from the atmosphere to the surrogate surfaces and does not include any possible surface resistance. Since limestone is not a perfect sink for SO_2, the deposition velocities to the stone surface will be lower than those measured using surrogate surfaces.

6. DISCUSSION

6a. *Airborne Concentrations of chemical Species*

The airborne concentration data have been analyzed statistically using a two sided t-test for averages. Significant differences in concentrations among the three sampling locations do not exist for any of the pollutants considered (Table 4).

The presence of a vertical concentration gradient requires that two conditions hold true. First, emissions from nearby sources must be sufficiently large to increase pollutant concentrations above the urban background level. Second, atmospheric mixing must be sufficiently small that vertical concentration differences can persist.

SO_4^{2-} and NO_3^- particles and HNO_3 gas are generally secondary pollutants that form from chemical reactions in the atmosphere (Seinfeld and Pandis, 1997). Therefore, on spatial scales corresponding to the height of the Cathedral, airborne concentrations of these species are expected to be spatially homogeneous since their formation is sufficiently slow to allow mixing, SO_4^{2-} and No_3^- are sometimes associated with coarse particles, in part due to sorption of SO_2 and HNO_3 onto alkaline soil dust (Wolff 1984). The absence of a concentration gradient in $S0_4^{2-}$ particles and total NO_3^- suggests that if these species are associated with coarse particles, there is adequate mixing to distribute them over the height of the Cathedral. The fact that elemental carbon does not exhibit a concentration gradient suggests that motor vehicle emissions from adjacent streets and the emissions from the nearby coal-fired steam plant are either rapidly mixed or else do not contribute significantly to concentrations at or above the fifth floor.

To investigate the extent of pollutant mixing near the building, a limited number of measurements of vertical wind speed were conducted on the fifth and sixteenth floor patios on five days during the term of this project. Results show the presence of strong vertical air motions along the walls of the building on all days tested. Although preliminary, these results provide qualitative evidence of vertical mixing as a consequence of wind impinging on the Cathedral.

6b. *Laser Particle Counts*

In the >0.5 μm size range, particle Counts by LPC do not show a significant difference between the fifth and sixteenth floors (Figures 7 and 8). However, >5 μm particle counts are on average 30% higher on the sixteenth floor than on the fifth floor Because of their greater inertia, sampling of large particles is more sensitive to factors such as inlet angle, flow characteristics in the inlet, and ambient wind direction. Therefore, the discrepancy in >5 μm concentrations between the two floors should be regarded with caution. Note that the chemical species data do not show a difference between the fifth and sixteenth floors: if the >5 μm particle concentrations are indeed slightly greater on the sixteenth floor, then it is unlikely that there is much SO_4^{2-}. NO_3^-, or carbon mass associated with these large particles.

Figures 7 and 8 both demonstrate that particle counts can vary considerably over the course of a day. In Figure 7, maxima and minima for >0 5 μm particle concentrations coincide well with those for >5 μm particles. This agreement between concentrations in the two particle sizes is found in most of the LPC data. However, changes in >0 5 μm particle concentrations are not well proportioned with those of >5 μm particles. The correlation coefficient for the data in Figure 7 is 0.41 whereas the 24-hour based correlation coefficients for all available LPC data range from-0.27 to 0.90 with a median value of 0.37. The low positive and occasional negative correlations are not surprising. Some meteorological parameters such as atmospheric stability may qualitatively affect >0 5 μm and >5 μm particle concentrations similarly. However, particles in these two size ranges are generally not emitted by the same sources and are not subjected to identical transport processes.

Table 3 shows that concentrations on Saturdays and Sundays are lower than those on weekdays. This is consistent with the expectation of reduced motor vehicle traffic and, possibly, reduced operations of some stationary sources on weekends in the Pittsburgh area.

6c. *Vertical Deposition Flux and Vertical Deposition Velocities*

There is considerable spatial variability in SO_2 deposition within each patio. However, most deposition velocities (V_d) are in the range 0.6-1.0 cm/s which is in agreement with unpublished data obtained previously at the Cathedral (Lutz et al., 1994; Etyemezian et al., 1995). The values are also in agreement

with measurements using the same method by Wu et al. (1992) on a bronze equestrian Statue in Gettysburg National Military Park. The greatest deposition velocities on the sixteenth floor correspond to locations 16a and 16c. The average deposition velocities for the full year are 0.85 ± 0.13 cm/s for the sixteenth floor compared with 0.69 ± 0.07 cm/s for the fifth floor. The sampling locations on the sixteenth floor are more exposed than those on the fifth floor which may, in part, be responsible for the slightly higher deposition velocities. Note that Sites 5a and 5f the most exposed sites on the fifth floor, have the highest deposition velocities on that floor. It is also of interest that the relative magnitudes of deposition velocity at one location with respect to another location do not change seasonally. For example, V_d is consistently higher at location 16c than it is at locations 5b, 5c, 5d, 5e. and 5f. Unpublished results of previous sampling at the Cathedral show a similar trend for SO_4^{2-} particle deposition (Gould et al., 1993; Lutz et al., 1994; and Etyemezian et al., 1995). These data also show that deposition fluxes of SO_4^{2-} particles to surrogate surfaces are usually at least a factor often lower than those for SO_2. In the earlier studies, surrogate surfaces for SO_4^{2-} particle and SO_2, gas collection were exposed on the fifth floor at five locations.

Locations 5f, 16a, and l6c are on parts of the building where there is no visible soiling. Location Sa is inside a 0.5 m heavily soiled indent on the wall. The portion of the wall immediately outside the indent and closer to the outer corner of the patio is clean. Overall, those sampling locations with the highest deposition velocities correspond to unsoiled parts of the building surface, and these are in relatively exposed areas. Furthermore, observations of the building during rainstorms suggest that these exposed areas also experience the most impingement by rain. Thus, we propose that deposition of pollutants and surface rain washing are processes in dynamic competition.

Archival photographs showing changes in soiling from the 1930's to the present support this hypothesis. These photographs show heavy soiling in the early years with decreasing amounts of soiling in more recent times. Examples of two photographs, from the late 1930's and from 1995, are shown in Figure II. The first photograph shows extensive soiling on the southwestern façade. In contrast, the later photograph shows that the top one-third of the building is virtually free of soiling, and that the demarcation line between soiled and unsoiled surfaces has receded on other parts of the building. Figure 12 indicates that the amount of annual precipitation has been roughly constant over these decades. However, airborne concentrations of SO_2, and particles have decreased steadily over the same time period (Davidson. 1979).

Thus, those areas of the façade that were soiled in the late 1930's have become unsoiled in recent years because the rate of removal of soiled material by rain washing is greater than the rate of soiling by pollutant deposition and chemical reaction. The earlier photograph suggests that the opposite was true in the late 1930's.

A study of the composition of the limestone on the Cathedral of Learning (McGee, 1997) supports the hypothesis that the soiling is a direct result of pollutant deposition. McGee has collected 37 samples of black, light, and red-brown surface material for examination by optical microscopy and electron scanning microscopy (SEM) with energy dispersive x-ray analysis of some samples. The black samples are composed primarily of $CaSO_4$ (gypsum) and contain numerous Fe-. Si-, and Al-rich fly ash particles. This is attributed to deposition of metal-containing particles and sulfur from pollutant sources in the area. The light surfaces are primarily calcite with only minor amounts of gypsum and metals. McGee reports that the microscopic and macroscopic appearance of light samples is similar to that of other limestone samples that are regularly washed either by rain or by routine cleaning. The color of the red-brown samples is attributed to rust from small metal spheres lodged in the stone, probably as a result of surface finishing of the limestone block.

It is of interest that one of the rainshields shown in Figure 4 was deployed in a soiled area on the fifth floor patio in January 1993; since then, the surface of the stone immediately above the rainshield has become cleaned by splashing raindrops (Figure 13). Clearly, the presence of this rainshield has caused a local disturbance in the balance between pollutant deposition and surface rain washing and has enhanced the amount of washing.

6d. Applicability of Results to Other Limestone Buildings

The absence of a vertical pollutant concentration gradient is probably due to a combination of factors that have implications for buildings in other areas. First, it is likely that vertical mixing is enhanced by the presence of the building; tall buildings in other areas may also have strong upward air motions that can deliver pollutants generated near the ground to upper levels. Second, the location of pollution sources around the Cathedral can greatly affect the airborne concentrations at the building. The Cathedral is located

in a major urban area with considerable local traffic as well as mobile and stationary sources for several kilometers in all directions. Thus, the contributions from nearby sources (within a few hundred meters) may be diminished by the presence of numerous regional pollution sources. Note that pollutants from several kilometers away have time to mix vertically in the atmosphere and can increase airborne concentrations at higher elevations. Effects of nearby sources may be more pronounced in cases where a building is located in a less polluted setting.

Third, the presence of nearby buildings is likely to have a major effect on dispersion near any building. The Cathedral is considerably taller than the surrounding buildings, and is 80 m from the nearest buildings to the north and west and over 120 m from the nearest buildings to the south and east. This isolation eliminates some of the trapping of pollutants that may occur in narrow street canyons, as reported by Lee and Park (1994).

It must be noted that no measurements in the present study were conducted below the fifth floor, and thus conclusions regarding the absence of a concentration gradient apply only above this level.

The concept of pollutant deposition and rain washing as competing processes has implications for other buildings. Comparing modem and archival photographs of the Cathedral shows general decreases in the soiling that are qualitatively consistent with decreases in pollutant concentration. Archival photographs of buildings where soiling is due to microbial activity may show distinctly different patterns.

7. SUMMARY AND CONCLUSIONS

In order to better understand pollutant sources and transport pathways responsible for the soiling of a tall limestone building, this study has investigated whether vertical gradients in airborne pollutant concentrations and deposition fluxes currently exist at the 42-story Cathedral of Learning in Pittsburgh, PA. The study has also considered long-term changes in soiling on the building as a means of identifying the roles of pollutant deposition and rain washing in affecting the soiling patterns.

The study involved measurements of airborne concentrations of SO_4^{2-} particles, elemental carbon particles. SO_2 gas, and total NO_3^- (NO_3^-; particles and HNO_3 gas) on the fifth floor, sixteenth floor, and roof. In addition. SO_2 deposition fluxes were measured on the fifth and sixteenth floors, and laser particle

counters were used on these same two floors to measure airborne particle number concentrations in two size ranges: >0.5 μm and >5 μm. The experiments were conducted for four weeks during each of the four seasons of the year beginning in fall 1995.

The airborne chemical species measurements indicate that there are no statistically significant vertical gradients for any of the pollutants. The lack of a gradient is attributed to a variety of regional and local sources that are expected to be well mixed by the time they reach the Cathedral, vertical winds in the vicinity of the building, and the lack of buildings nearby that might otherwise trap pollutants and prevent vertical mixing. The laser particle counts for >0.5 μm particles likewise show lack of gradient, although the >5 μm particles show slightly greater airborne particle number concentrations on the sixteenth floor compared with those on the fifth floor.

Deposition fluxes and deposition velocities of SO_2 to surrogate surfaces show small but consistent differences among the locations sampled. Values are greatest at locations that are most exposed to the wind such as the outside corners of the patios. The values are greater on the sixteenth floor than on the fifth floor, partly because two of the three sixteenth floor sampling locations are situated on the corners of the patio.

Comparison of archival with more recent photographs shows that the soiling on the Cathedral has decreased over time. This is consistent with decreasing trends in airborne pollutant concentrations over the past several decades. It is thus likely that rain is washing soiled material off the building surface at a greater rate than chemical species are depositing and reacting with the surface. The opposite apparently was true in the 1930's when air pollutant concentrations were considerably greater than at present.

Overall, these results may be of interest to conservators who must develop strategies for cleaning and restoring building surfaces and for preventing future damage. Although the conclusions reached here are a result of testing at the Cathedral of Learning, it is likely that many of the findings also apply to buildings in other urban areas.

8. ACKNOWLEDGMENTS

This research was funded by the National Park Service Cooperative Agreements 042419005 and 00196035.
The assistance of the Department of Facilities Management at the University of Pittsburgh and Dominic

Fagnelli, the Cathedral of Learning building engineer, are greatly appreciated. The authors wish to acknowledge Susan Sherwood for her valuable suggestions and assistance over the past several years. Thanks are due to Michael Lutz and Timothy Gould for their earlier work on the Cathedral and to Mitchell Small for help with the statistical analysis. The authors also wish to thank Spyros Pandis, Hampden Kuhns, Weiping Dai, Maria Zufall, and Ross Strader for their frequent and welcome suggestions. Chandra Reedy and Elizabeth Bede provided comments and insights that were very helpful in the writing of this manuscript. A large fraction of the airborne sampling setup was constructed by Larry Cartwright and his crew. Karen Pinkston and Preshanth Mekala contributed their time to ion chromatography analyses. The historical photograph was furnished by the Carnegie Library of Pittsburgh, Oakland Branch. Justin Parkhurst assisted with the collection of several historical photographs. The computer drawings of the Cathedral that appear in Figure 2 were created by Judy Lee and modified by Ivan Locke, Sean Jutahkiti, Anthony Paul, and Thomas Curry are thanked for their work on measuring vertical wind speeds near the walls of the Cathedral of Learning.

9. REFERENCES

Amoroso, G.G., and V. Fassina. 1983. Stone Decay and Conservation: Atmospheric Pollution, Cleaning, Consolidation and Protection. *Materials Science Monographs* 11, Elsevier, 1983.

Appel, B.R., Y. Tokiwa, and M. Haik. 1981. Sampling of Nitrates in Ambient Air. *Atmospheric Environment* 15: 283-289.

Bock, E. and W. Sand. 1993. A Review: The Microbiology of Masonry Deterioration .*Journal of Applied Bacteriology* 74: 503-514.

Braun, R.C., and M.J.G. Wilson. 1970. The Removal of Atmospheric Sulphur by Building Stones. .*Atmospheric Environment* 4: 371-378.

Cadle, S.H., and P..A. Mulawa. 1987. The Retention of SO_2 by Nylon Filters. *Atmospheric Environment* 21: 599-603.

Chan, W.H., D.B. Orr, and D.H.S. Chung. 1986. An Evaluation of Artifact SO_4^{2-} Formation on Nylon Filters Under Field Conditions. *Atmospheric Environment* 20: 2397-2401.

Chow, J.C., J.G. Watson, L.C. Pritchet, W.R. Pierson, C..A. Frazier, and R.G. Purcell. 1993. The DR.I Thermal/Optical Reflectance Carbon Analysis System: Description, Evaluation, and Applications in U.S. Air Quality Studies. *Atmospheric Environment* 27a: 1185-1201.

Dabberdt, W.F., and W.G. Hoydysh. 1991. Street Canyon Dispersion: Sensitivity to Block Shape and Entrainment. *Atmospheric Environment* 25a: 1143-1153.

Davidson. C.I. 1979. Air Pollution in Pittsburgh: A Historical Perspective. *Journal of the Air Pollution Control Association* 29: 1035-1041.

Davidson. C.I., S.E. Lindberg. J.A. Schmidt, L.G. Cartwright, and L.R. Landis. 1985. Dry Deposition of Sulfate Onto Surrogate Surfaces. *Journal of Geophysical Research* 90:. 2123-2130.

Del Monte. M., C. Sabbioni, and O. Vittori, 1981. Airborne Carbon Particles and Marble Deterioration. *Atmospheric Environment* 15: 645-652.

DePaul, F.T., and C..M. Sheih. 1986. Measurements of Wind Velocities in a Street Canyon. *Atmospheric Environment* 20: 455-459.

Etyemezian, V., C.I. Davidson, S. Finger et al. 1995. Influence of Atmospheric Pollutants on Soiling of a Limestone Building Surface. Progress Report for the National Park Service. September, 1995.

Fenter, F.F., C. Francois, and M..J. Rossi. 1995. Experimental Evidence for the Efficient "Dry Deposition" of Nitric Acid on Calcite. *Atmospheric Environmental* 29: 3365-3372.

Freemantle, M. 1996. Historic Monuments Pose Challenge to Conservation Scientists. *Chemical and Engineering News* 74: 20-23.

Gould, T.R., C.I. Davidson, S. Finger et al. 1993. Influence of Atmospheric Pollutant Concentrations and Deposition Rates on Soiling of a Limestone Building Surface Progress Report for the National Park Service. May, 1993.

Haneef, S.J., J..B. Johnson, C. Dickinson, G.E. Thompson, and G.C. Wood. 1992. Effect of Dry Deposition of NO_x and SO_2 Gaseous Pollutants on the Degradation of Calcareous Building Stones *Atmospheric Environment* 26a: 2963-2974.

Hering, S.V. et al. 1988. The Nitric Acid Shootout Field Comparison of Measurement Methods. *Atmospheric Environment* 22: 1519-1539.

Hoydysh, W G., and W..F. Dabberdt. 1994. Concentration Fields at Urban Intersections: Fluid Modeling Studies. *Atmospheric Environment* 28: 1849-1860.

Huber, A.H., S. Pal Arya, S.A. Rajala, and J.W. Borek. 1991. Preliminary Studies of Video Images of Smoke Dispersion in the Near Wake of a Model Building. *Atmospheric Environment* 25a: 1199-1209.

Hutchinson, A.J., J.B. Johnson, G.E. Thompson. G. C. Wood. P.W. Sage, and M.J. Cooke. 1992. The Role of Fly-ash Particulate Material and Oxide Catalysts in Stone Degradation. *Atmospheric Environment* 26a: 2795-2803.

Hutchinson, A.J., J.B. Johnson, G.E. Thompson, G.C. Wood, P.W. Sage, and M.J. Cooke. 1993. Stone Degradation Due to Wet Deposition of Pollutants. *Corrosion Science* 34: 1881-1898.

Johansson. L.G., O. Lindqvist, and R.E. Mangio. 1988. Corrosion of Calcareous Stones in Humid Air Containing SO_2 and NO_2. *Durability of Building Materials* 5*:* 439-449.

Judeikis, H.S., T.B. Stewart, and A.G. Wren. 1978. Laboratory Studies of Heterogeneous Reactions of SO_2. *Atmospheric Environment* 12: 1633-1641.

Kirkitsos, P., and D. Sikiotis. 1995. Deterioration of Pentelic Marble, Portland Limestone and Baumberger Sandstone in Laboratory Exposures to Gaseous Nitric Acid. *Atmospheric Environment* 29: 77-86.

Lee, J.T., D.L. Call, R.E Lawson Jr., W.E. Clements, and D.E. Hoard. 1991. A Video Image Analysis System for Concentration Measurements and Flow Visualization in Building Wakes. *Atmospheric Environment* 25a: 1211-1225.

Lee, I.Y., and H.M. Park. 1994. Parametrization of the Pollutant Transport and Dispersion in Urban Street Canyons. *Atmospheric Environment* 28: 2343-2349.

Livingston, R.A. 1992. Graphical Methods for Examining the Effects of Acid Rain and Sulfur Dioxide on Carbonate Stones. *Proceedings of the 7th International Congress on Deterioration and Conservation of Stone*. Lisbon, Portugal. 1992. 375-386.

Lutz, M.R., C.I. Davidson, S. Finger et al. 1994. Influence of Atmospheric Pollutants on Soiling of a Limestone Building Surface 1991-1994. Progress Report for the National Park Service. September, 1994.

McGee, E.S. 1995. Sampling Protocol Used at the Cathedral of Learning in Pittsburgh, Pennsylvania. USGS Open-File Report 95-672.

McGee, E.S. 1997. Surficial Alteration at the Cathedral of Learning in Pittsburgh, Pennsylvania. USGS Open-File Report 97-275.

Meierding, T.C. 1993. Marble Tombstone Weathering and Air Pollution in North America. *Annals of the Association ofAnierican Geographers* 83 (4): 568-588.

Mitchell, J D. Gu.R., T.E. Ford, and N.S. Berke. 1996. Fungal Degradation of Concrete. *DECHEMA Monographs* 133: 135-142.

Mossotti, V.G., and A.R. Eldeeb. 1994. Calcareous Stone Dissolution by Acid Rain. Manuscript in progress. Version-0.7, Dec. 12, 1994.

Mulawa, P.A., and S.H. Cadle. 1985. A Comparison of Nitric Acid and Particulate Nitrate Measurements by the Penetration and Denuder Difference Methods. *Atmospheric Environment* 19: 1317-1324.

Palmer et al. 1991 as cited in Bock and Sand (1993). Palmer, R.J., J. Siebert, and P. Hirsch 1991. Biomass and Organic Acids in Sandstone of a Weathering Building: Production by Bacterial and Fungal Isolates. *Microbial Ecology* 21: 253-266.

Qin, Y., and S.C. Kot. 1990. Validation of Computer Modeling of Vehicular Exhaust Dispersion Near a Tower Block. *Building and Environment* 25*:* 125-131.

Qin, Y., and L.Y. Chan. 1993. Traffic Source Emission and Street Level Air Pollution in Urban Areas of Guangzhou, South China (P.R.C.). *Atmospheric Environment* 27b: 275-282.

Qin, Y., and S.C**.** Kot 1993. Dispersion of Vehicular Emission in Street Canyons, Guangzhou City, South China (P.R C.). *Atmospheric Environment* 27b: 283-291.

Sabbioni, C. 1994. Effects of Air Pollution on Historic Buildings and Monuments. Scientific Basis for Conservation: Physical. Chemical, and Biological Weathering. *European Cultural Heritage Newsletter on Research* 8(1): 2-6.

Seinfeld, J.H., and S.N. Pandis. 1997. *Atmospheric Chemistry Air Pollution to Global Change.* John Wiley and Sons, 1997 (in press).

Sherwood, S.I., D.A. Gatz, R.P. Hosker Jr. et al. 1990. Processes of Deposition to Structures. NAPAP SOS/T Report 20 in *National Acid Precipitation Assessment Program. Acidic Deposition: State of Science and Technology. Volume III.* September 1990.

Spedding, D.J. 1969. Sulphur Dioxide Uptake by Limestone. *Atmospheric Environment* 3*:* 683.

Spiker, E.C., R.P. Hosker Jr., V.C. Weintraub, and S.I. Sherwood. 1995. Laboratory Study of SO_2 Dry Deposition on Limestone and Marble: Effects of Humidity and Surface Variables. *Water, Air, and Soil Pollution Proceedings of the 1995 5th International conference on Acidic Deposition: Science and Policy. Acid Reign 95,* Goteberg, Sweden. 1995. 2679-2685.

Tayler, S., and E. May 1991. The Seasonality of Heterotrophic Bacteria on Sandstones from Ancient Monuments. In *Biodeterioration of Cultural Property* ed. R.J. Koestler, Elsevier, New York, NY. 390-391.

Thompson, R.S. 1993. Building Amplification Factors for Sources Near Buildings:A Wind Tunnel Study. *Atmospheric Environment* 27a: 2313-2325.

Warscheid, T., M. Oelting, and W.E. Krumbein. (1991). Physico-chemical Aspects of Biodeterioration Processes on Rocks with Special Regard to Organic Pollutants. In *Biodeterioration of Cultural Property* ed. R.J. Koestler, Elsevier, New York. NY. 397-399.

Wilmzig, M., and E. Bock 1995. Endangerment of Mortars by Nitrifiers, Heterotrophic Bacteria and Fungi. In *Biodeterioration and Biodegradation* 9 eds. A. Bousher et al., Institution of Chemical Engineers, Rugby, UK, 195-197.

Winkler, E.M. 1996. Important Agents of Weathering for Building and Monumental Stone. *Engineering Geology* 1:381-400.

Wolff, G.T. 1984. On the Nature of Nitrate in Coarse Continental Aerosols *Atmospheric Environment* 18: 977-981.

Wu, Y.L., C.I. Davidson, D.A Dolske, and S.I. Sherwood. 1992. Dry Deposition of Atmospheric Contaminants:The Relative Importance of Aerodynamic, Boundary Layer, and Surface Resistances. *Aerosol Science and Technology* 16: 65-81.

Young, P. 1996a. Pollution-Fueled “Biodeterioration” Threatens Historic Stone *Environmental Science and Technology* 30: 206a-208a.

Young, P. l996b. Mouldering Monuments. *New Scientist* 152: 37-38.

Zappia, G., C. Sabbioni, and G. Gobbi. 1993. Non-Carbonate Carbon Content on Black and White Areas of Damaged Stone Monuments. *Atmospheric Environment* 27a: 1117-1121.

10. SUPPLIERS OF EQUIPMENT

1. Clean Room Products Inc., 1800 Ocean Avenue, Ronkonkoma, NY 11779-6532.

2. Costar, One Alewife Center, Cambridge, MA 02140.

3. Dionex Corp., 1228 Titan Way, Sunnyvale, CA 94088-3603.

4. Fisher Scientific, 711 Forbes Avenue, Pittsburgh, PA 15219-4785.

5. Gelman Sciences, 600 South Wagner Road, Ann Arbor, MI 48106.

6. Hoke, One Tenakill Park, Cresskill, NJ 07626.

7. Millipore Corp., 80 Ashby Road, Bedford, MA 01730.

8. Pallflex Corp., 125 Kennedy Drive, Putnam, CT 06260.

9. Savillex Corp., 6133 Baker Road, Minnetonka, MN 55345.

10. Singer Corp., product division closed.

11. TSI Inc., P.O. Box 64394, St Paul, MN 55164.

12. Whatman, 9 Bridgewell Place, Clifton, NJ 07014.

11. AUTHOR BIOGRAPHIES

Vicken Etyeinezian is a doctoral student at Carnegie Mellon University (CMU). He received combined bachelor degrees in physics and engineering from Occidental College and Caltech, respectively and an MSE in environmental engineering from the Johns Hopkins University. His research has focused on the effects of atmospheric pollutants on sensitive building materials, with an emphasis on dry deposition and surface rain washing. Some of his other interests include policies for sustainable environments in developing countries, urban and remote atmospheric chemistry, contaminant transport in groundwater, and innovative solutions for wastewater treatment.

Cliff I. Davidson is Professor of Civil and Environmental Engineering/Engineering and Public Policy at Carnegie Mellon University (CMU). He is also Director of the Environmental Institute at CMU. His main research interests involve atmospheric pollutants, focusing on the way particles and gases are transported through the atmosphere, the mechanisms by which particles and gases deposit from the atmosphere onto different types of surfaces, and historical trends in air pollution levels. His main educational activities include developing material that can be used broadly in basic science and engineering courses to increase student awareness of environmental issues.

Susan Finger is on the faculty of the Civil and Environmental Engineering Department at Carnegie Mellon University. She is also affiliated with the Engineering Design Research Center, the Robotics Institute, and the Department of Mechanical Engineering. She is a founder and Co-Editor-in-Chief of the journal Research in Engineering Design. Dr. Finger’s research interests include representation languages for designs, integration of design and manufacturing concerns and computer-aided engineering.

Barabas Noemi received a BS degree in chemical engineering and public policy with a minor in environmental engineering from Carnegie Mellon University. She is completing work on a master’s degree (with subsequent Ph.D.) in Environmental Engineering in the Water Resources and Environmental

Engineering Program at the University of Michigan. Her interests are water resource management and policy and its application in Eastern Europe.

Mary F. Striegel currendy serves as the Materials Research Program Coordinator for the National Center for Preservation Technology and Training, where she is responsible for the supervision of in-house and external research on the effects of air pollution on cultural resources. Before coming to NCPTT, Mary was a researcher with the Getty Conservation Institute. She holds bachelor degrees in fine arts and chemistry from the University of Louisville, a masters degree in analytical chemistry from Indiana University-Purdue University in Indianapolis, and a doctoral degree in inorganic chemistry from Washington University in St. Louis.

Dr. Judith C. Chow, Research Professor in the Energy and Environmental Engineering Center (EEEC) at the Desert Research Institute (DRJ). University and Community College System of Nevada, has over 19 years of experience in conducting air quality studies and performing statistical data analysis. She directs DRI's Environmental Analysis Facility where she supervises filter processing and chemical operations. In this capacity, she has developed cost-effective, yet accurate, methods for sampling and analysis. Dr. Chow has gained extensive experience in program planning: ambient and source sampling from urban and non-urban areas; gravimetric, x-ray fluorescence, atomic absorption spectrophotometric, ion chromnatographic, automated colorimetric, and thermal/optical reflectance carbon analyses of filter samples, as well as interpretative statistical data analyses, principal component analyses, such as multivariate statistical analysis, and chemical mass balance receptor modeling: data interpretation: and reporting.

12. LIST OF TABLES

13. LIST OF FIGURES

Figure 8a. Daily Average, Maximum, and Minimum Laser Particle Counts for> 0.5 µrn Particles.

Maxima on 2/21.2/22,2/23,2/27/96 are 107, 133, 146, 109 particles/cm^3, respectively. Minima on 2/24, 5/27, 5/29, and 7/26/96 are 0.90, 0.66, 0.97, and 0 86 particles/cm^3, respectively Vertical bars extend from minimum to maximum measured concentrations.

Figure 8b. Daily Average. Maximum, *and* Minimum Laser Particle Counts for> 5 urn Particles.

Maxima on 2/21,2/22.,2/23,2/27, and 8/13/96 are 1.38, 10.01,20.35, 1.33, and 3.78 particles/cm^3, respectively. Vertical bars extend from minimum to maximum measured concentrations.

Figure 9. SO_2 Deposition fluxes.

Figure 10. SO_2 Deposition Velocities.

Figure 11. The Cathedral of Learning 1930's and Present.

The photograph on the left was taken C, late 1930's (courtesy of the Carnegie Library of Pittsburgh, Oakland Branch. Pittsburgh, PA) whereas the photograph on the right was taken in 1995. A comparison of the areas within the circles illustrates how surface soiling at some locations on the building has decreased. This soiling is due to deposition and chemical reaction of air pollutants on the limestone surface.

Figure 12. Annual Precipitation for Pittsburgh.

The numbers on the x-axis represent the middle year of the ten year period used to obtain the average annual precipitation shown Data were obtained from the National Climatic Data Center Web page.

Figure 13. Washing of a Soiled Surface at the Cathedral by Raindrops Impinging on a Rainshield.

The rainshield shown was mounted on the wall of the Cathedral in January 1993. The photograph above was taken in September 1997. The portion of the wall above the rainshield has been cleaned by raindrops impinging on the top surface of the rainshield.

Table 1. Etyemezian et al.

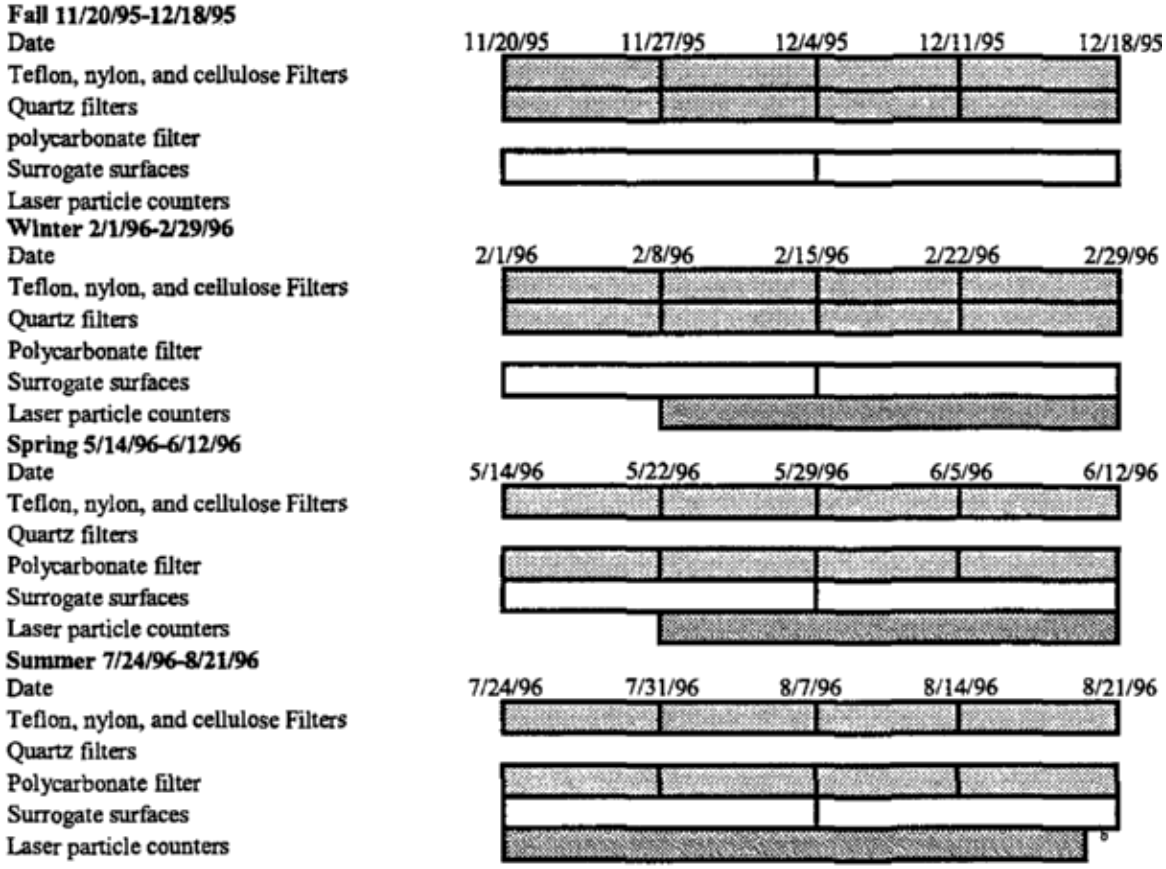

[a] A vertical line indicates a sample change.
[b] No data past 8/16/96

Table 2. Eyemezian et al.

Filter Type	Analyte[a]	Analytical detection limit (µg on filter)	Average sample mass (µg)	Average Field Blank mass (µ&g)
Teflon	NO_3^-	0.2	18.9	0.92
	SO_4^{2-}	0.2	56.2	0.43
Nylon	NO_3^-	0.2	28.0	0.47
	SO_4^{2-}	0.2	19.2	0.59
Cellulose	SO_4^{2-}	0.9	284	1.4
Cellulose Backup	SO_4^{2-}	0.9	20.9b	1.0
Quartz	Elemental Carbon	0.6	70.5	0.30
Cellulose Vertical	SO_4^{2-}	0.9	2830	2.5

[a] Teflon filters collected NO_3^- and SO_4^{2-} particles, while nylon filters collected HNO_3 and small amounts of SO_2. Cellulose filters collected SO_2.

[b] Average excludes Backup filters that were not found to be different from the blank at 95% confidence

Table 3. Etyemezian et al.

Sampling Period	Average concentrations of >0.5 μm particles (particles/cm^3)			Average concentrations of >5 μm particles x 100 (particles/cm^3)		
	Weekdays	Saturdays	Sundays	Weekdays	Saturdays	Sundays
2/8/96 - 2/29/96	24.1	14.4	5.2	8.86	0.68	0.76
5/22196 - 6/12/96	14.2	11.7	7.9	1.02	0.75	0.36
7/24/96 - 8/16/96	23.5	12.8	14.6	0.50	0.39	0.29

Table 4 Etvemezian et al

Chemical Species	P-values for 5th floor and 16th floor	P-values for 5th floor and roof	P-values for 16th floor and roof
SO_4^{2-}	0.953	0.993	0.959
total NO_3^-	0.981	0.478	0.500
SO_2	0.375	0.539	0.895
Elemental carbon	0.897	0.518	0.451

[a] In order for two sets of data to have significantly different mean values (in a statistical sense), the P-value has to be lower than unity minus the confidence of the test. For example, to show that mean concentrations for a chemical species on the 5th floor are different than those on the 16th floor with 95% confidence, the P value would have to be less than 0.05 (1-0.95).

Figure 1. Etyemezian et al.

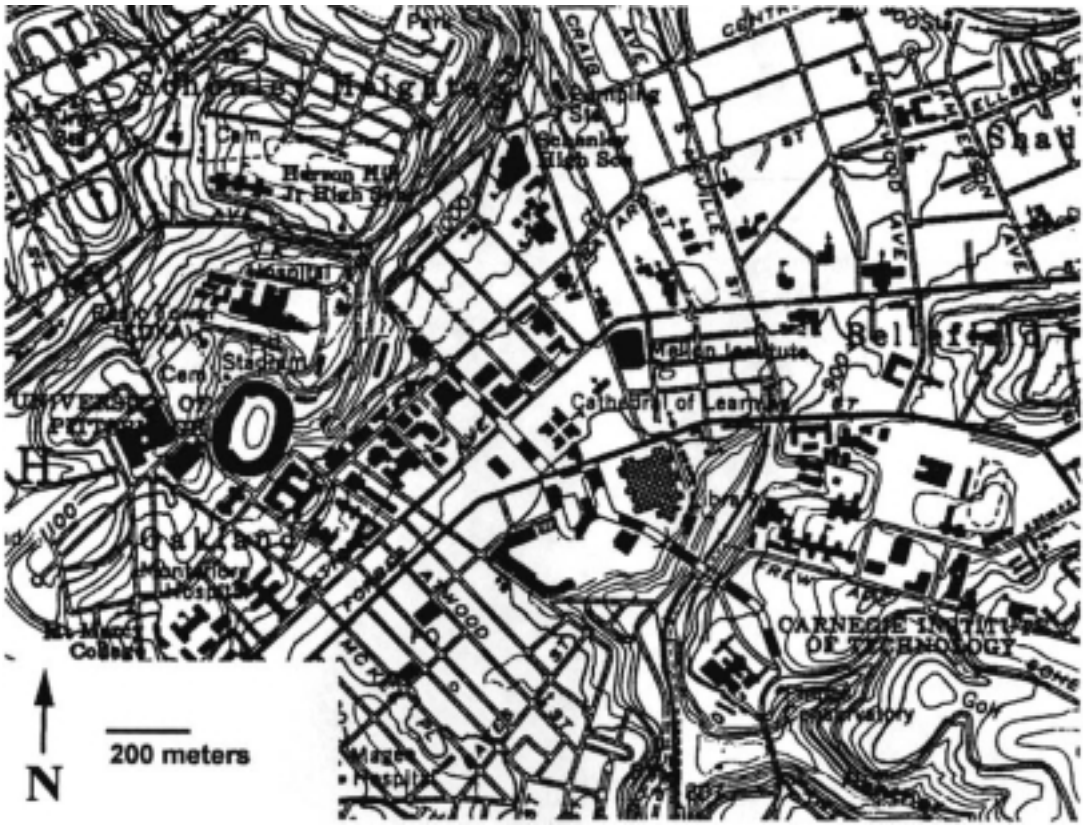

Figure 2. Etyemezian et al.

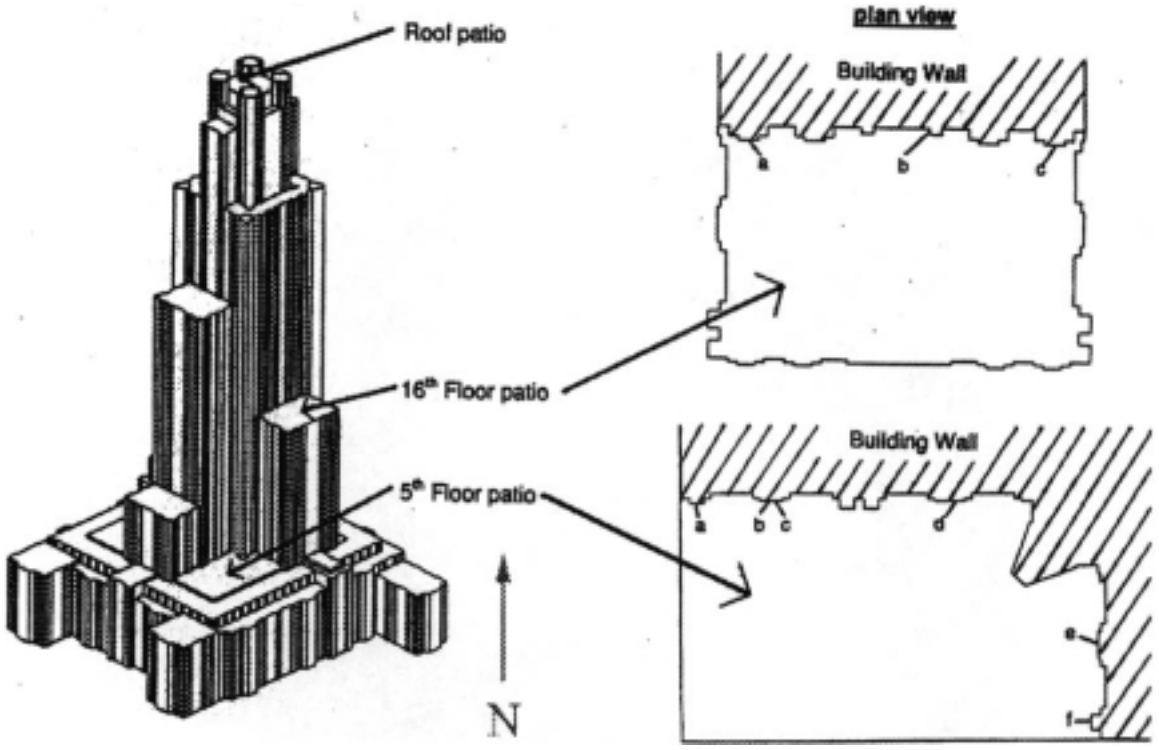

Figure 3a. Etyemezian et al.

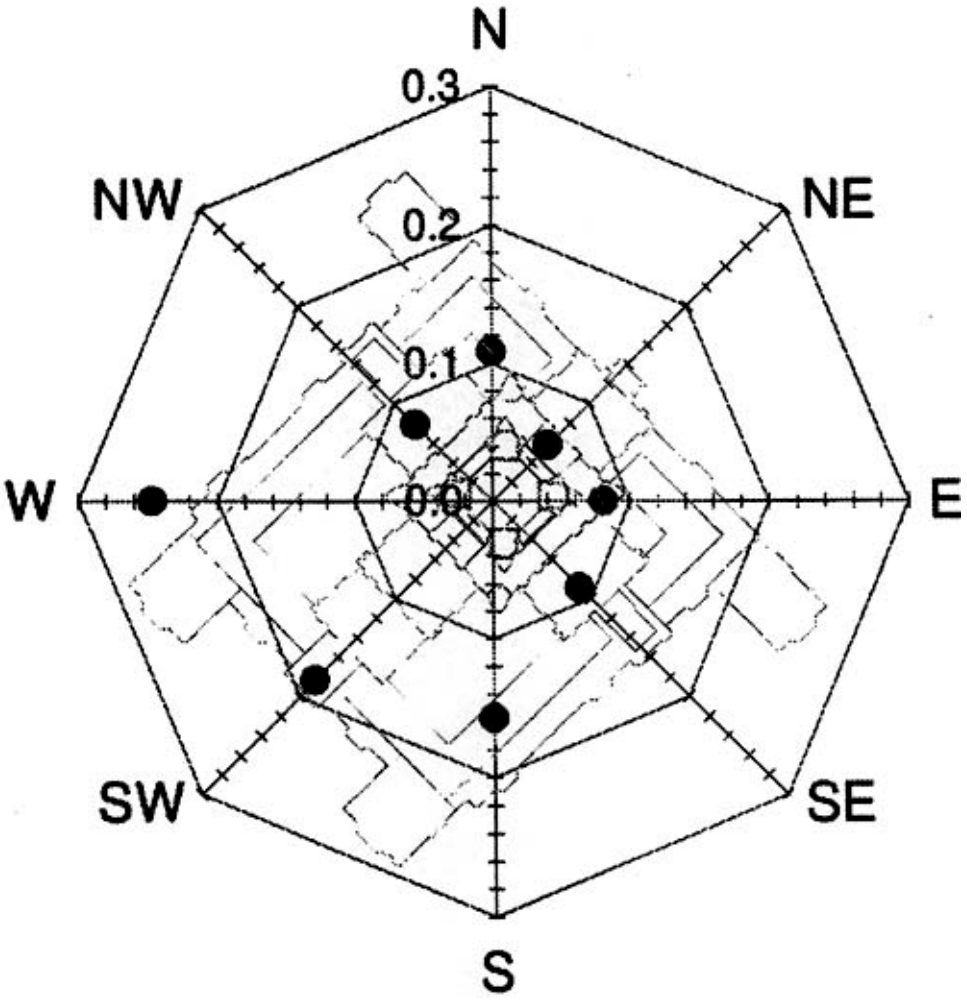

Figure 3b. Etyemezian et al.

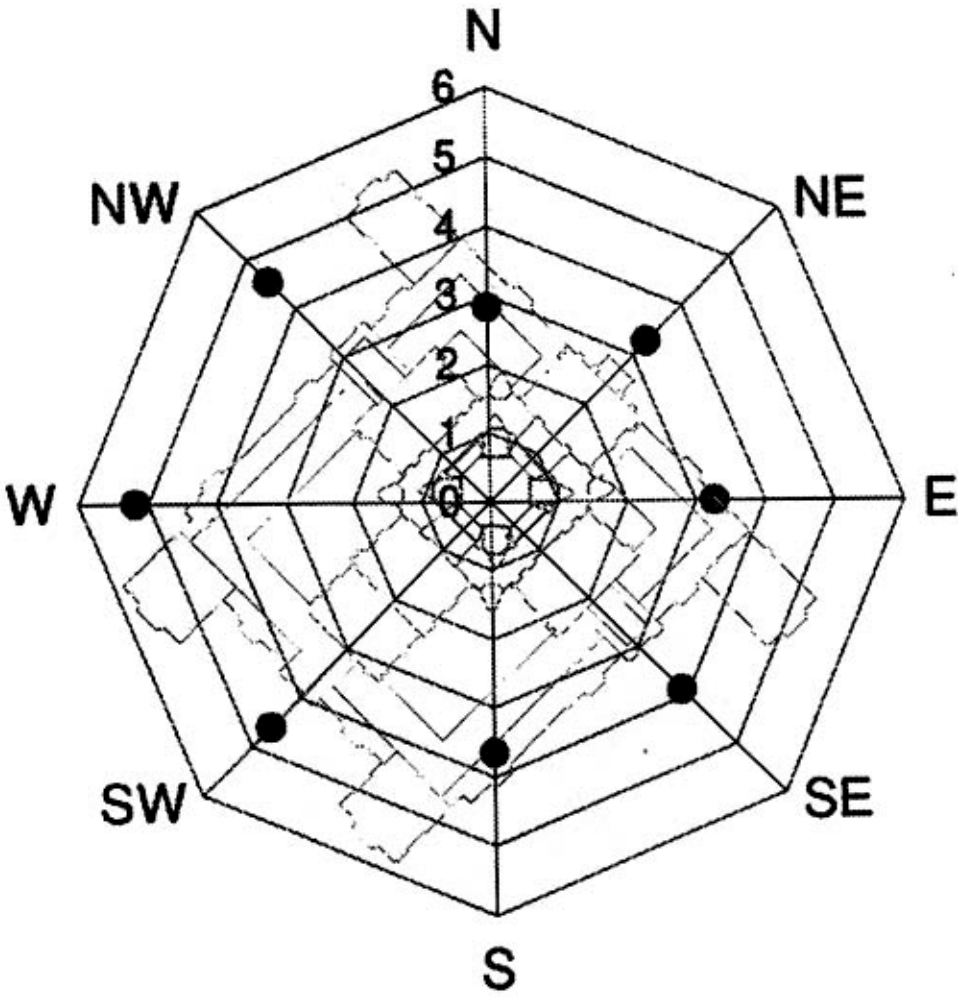

Figure 4. Etyemezian et al.

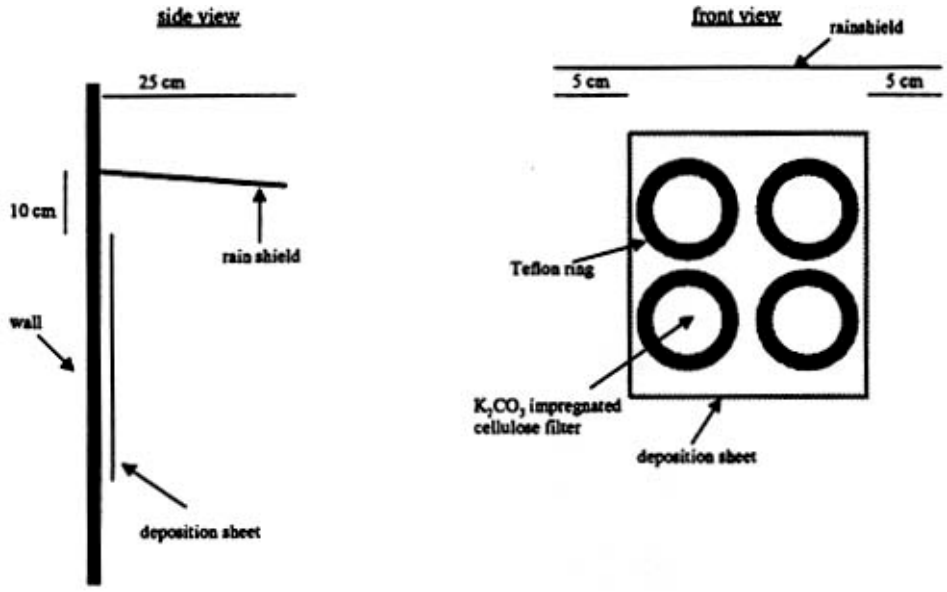

Figure 5. Eyemezian et al.

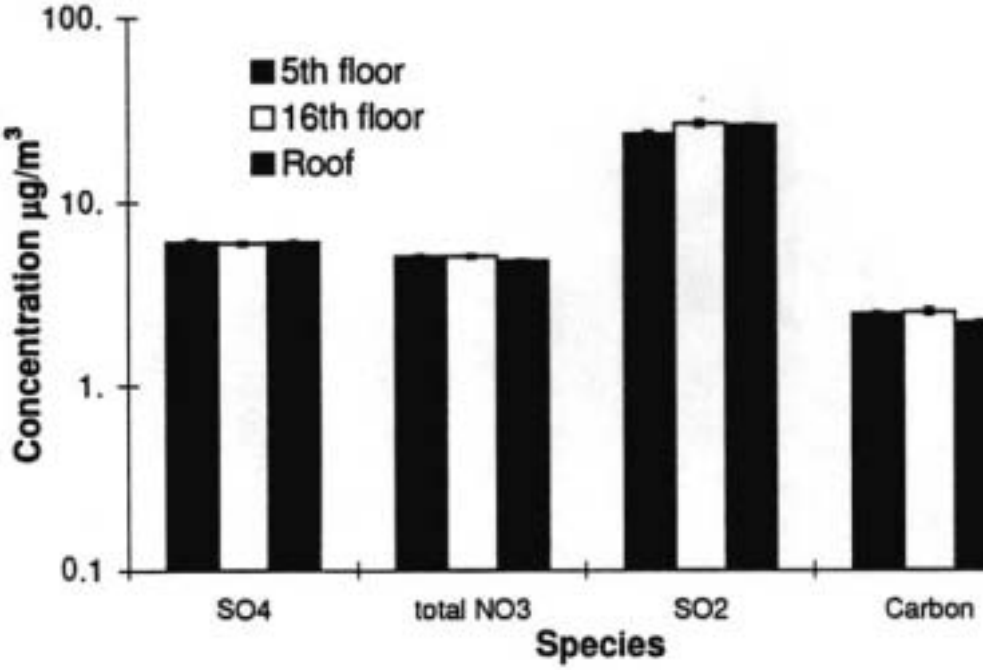

Figure 6. Etyemezian et al.

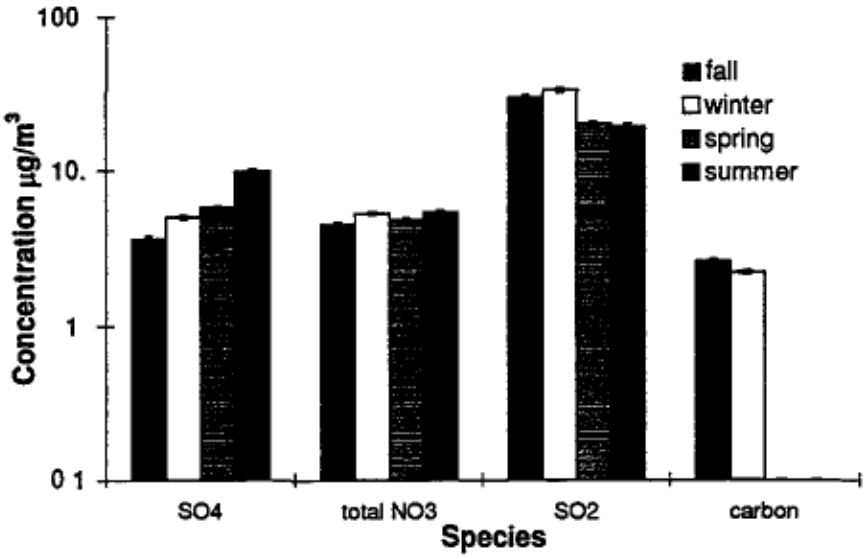

Figure 7a. Etyemezian et al.

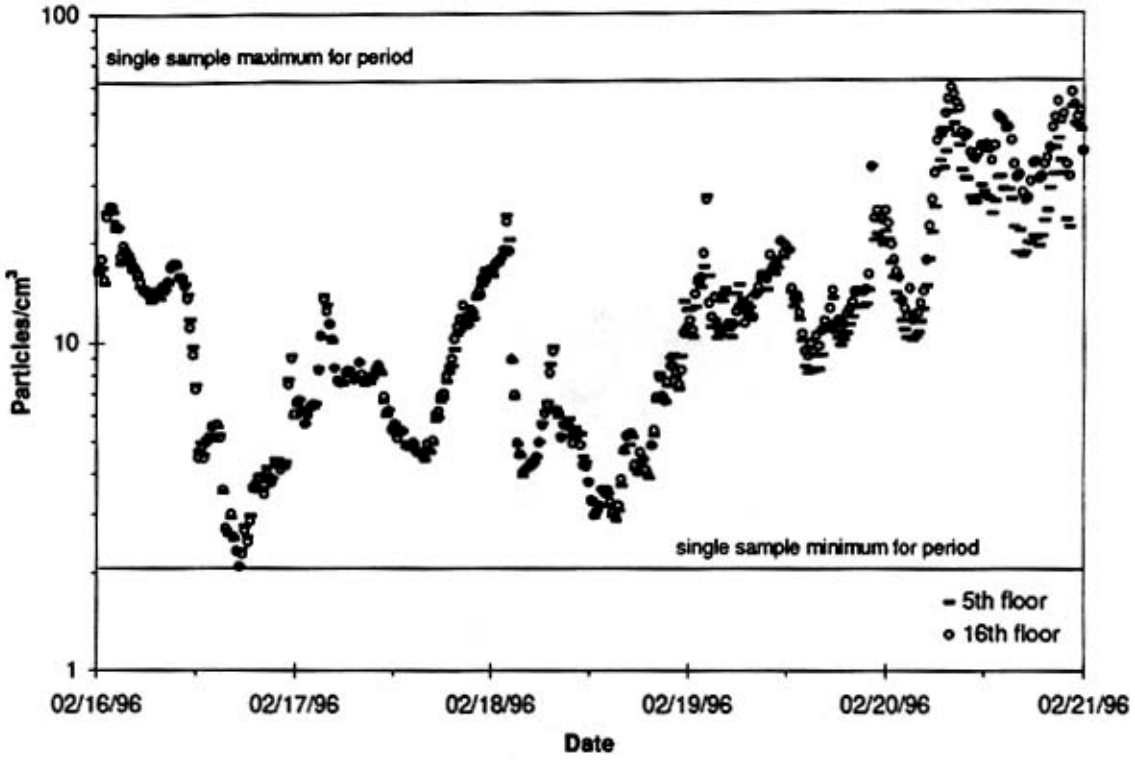

Figure 7b. Etyemezian et al.

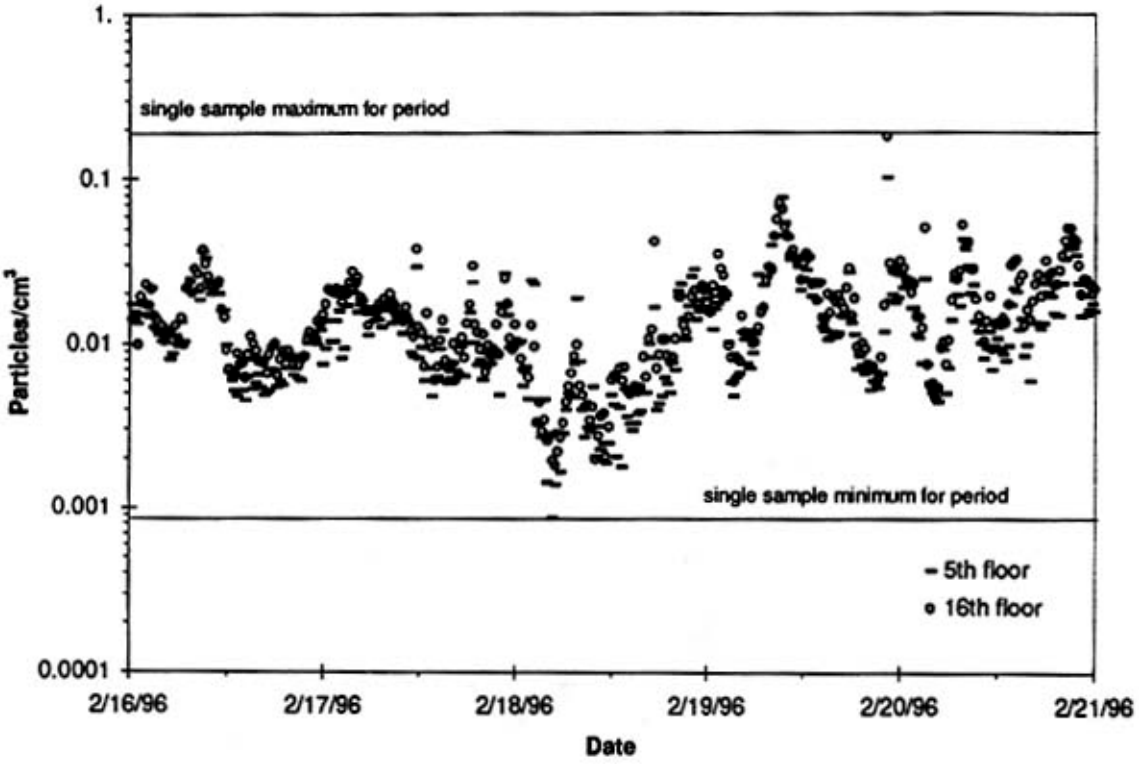

Figure 8a. Etyemezian et al

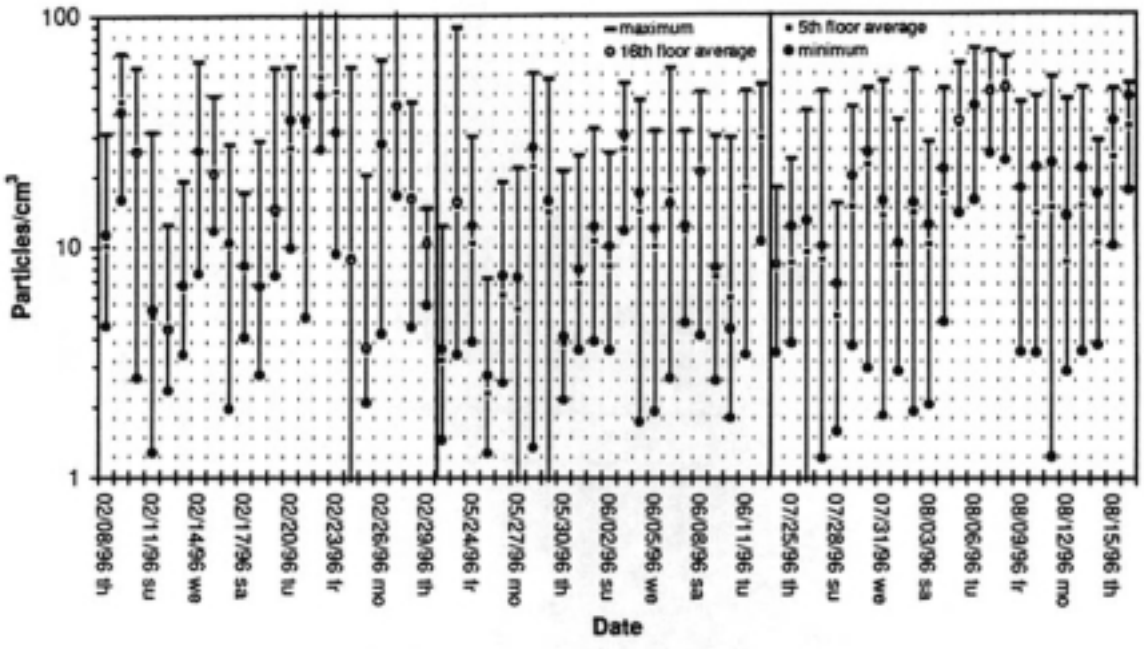

Figure 8b. Etyemezian et al.

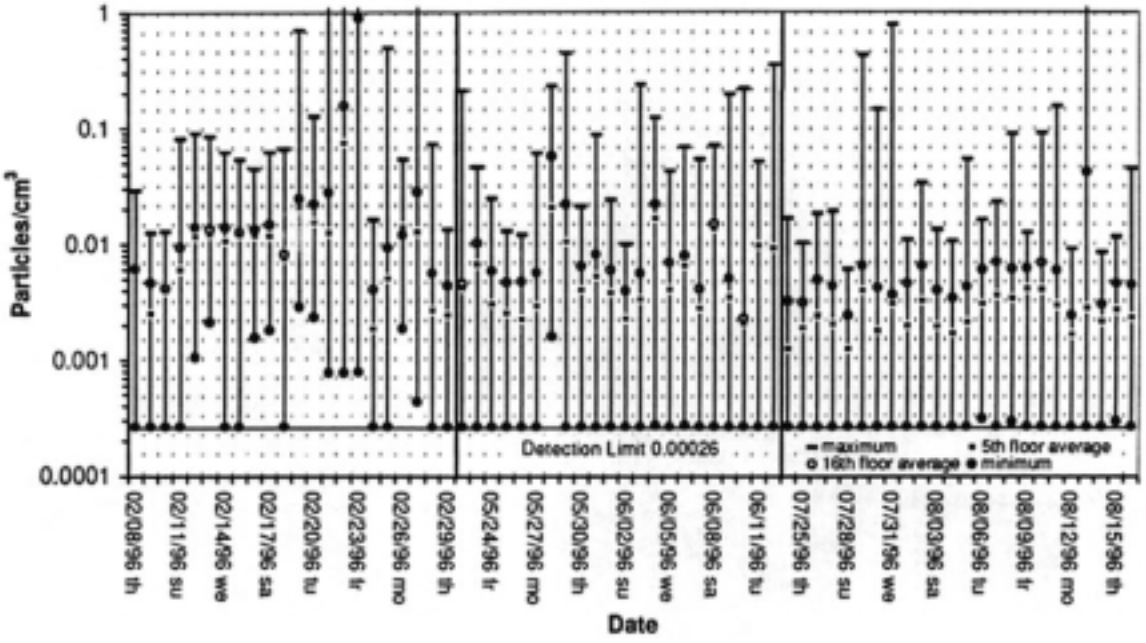

Figure 9. Etyemezian et al.

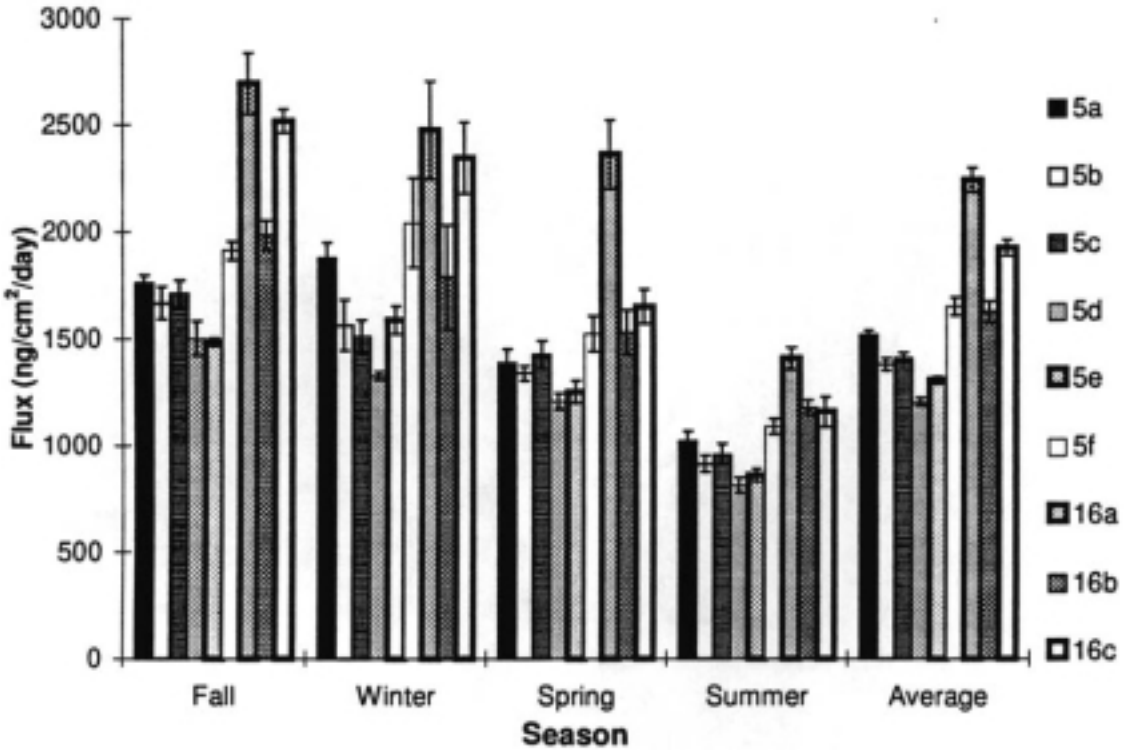

Figure 10. Etyemezian et al

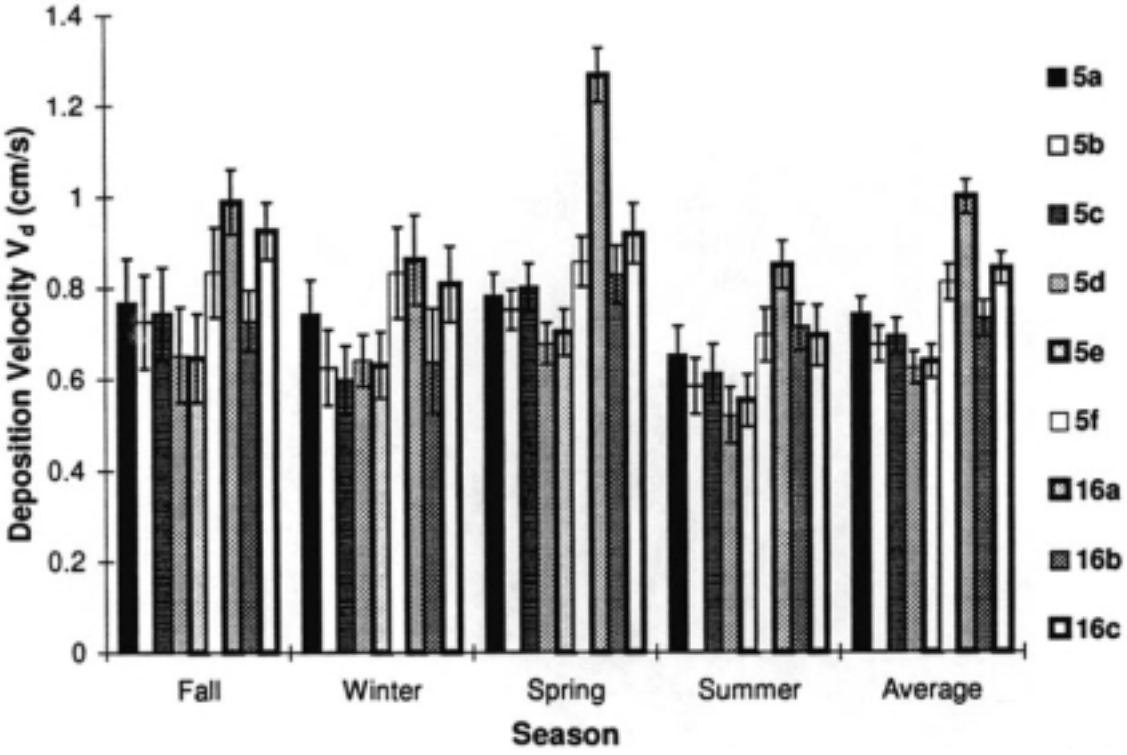

Figure 11. Etyemezian et al.

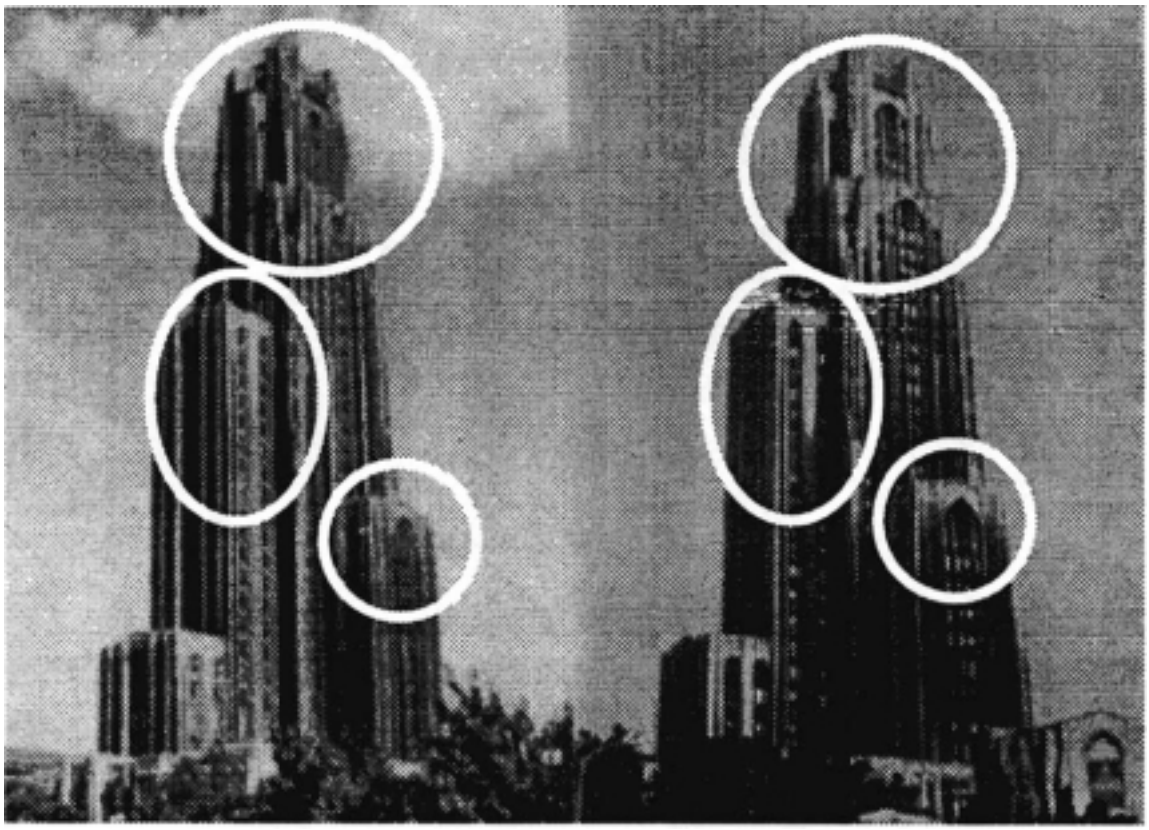

Figure 12. Etyemezian et al.

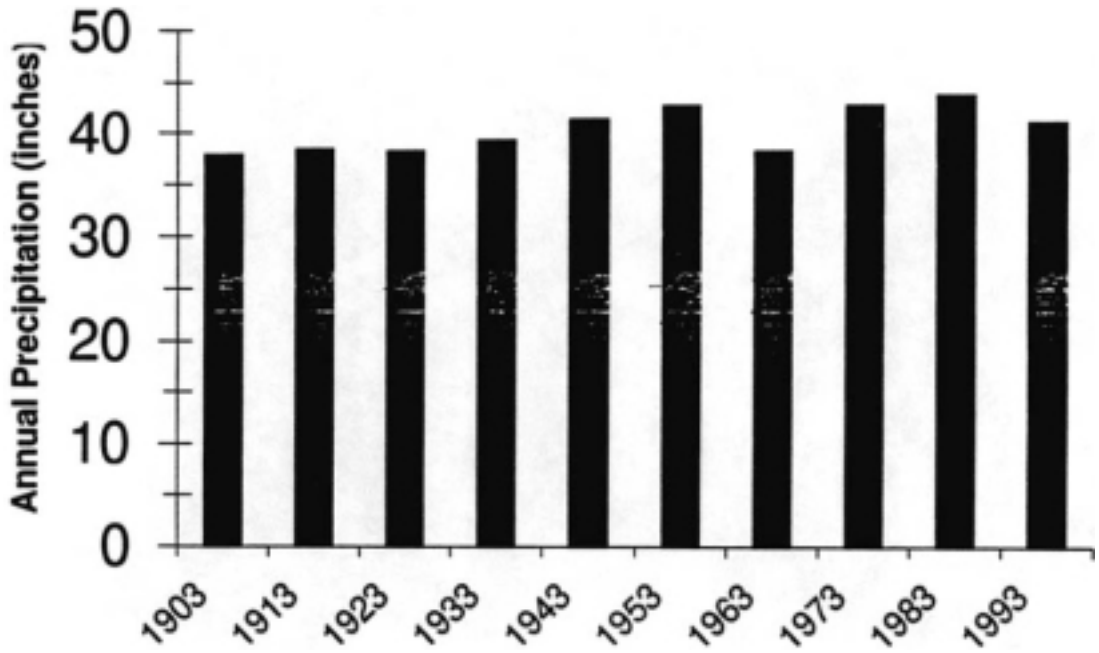

Figure 13. Etyemezian et al.